IN THE UNITED STATES PATENT AND TRADEMARK OFFICE

In Re the Application of:	Group Art Unit: 1647
COX et al.	Examiner: Lee, Betty L.
Serial No.: 10/031,154	DECLARATION OF GEORGE N. COX, III (Under 37 CFR 1.132)
Filed: January 14, 2002	
Atty. File No.: 4152-3-PUS	
For: "IMMUNOGLOBULIN FUSION PROTEINS"	

Commissioner for Patents
P.O. Box 1450
Alexandria, VA 22313-1450

Dear Sir:

I, George N. Cox, III, declare as follows:

1. I am a co-inventor of the above-referenced patent application and am familiar with the application. I am a skilled artisan in the fields of molecular and cellular biology.

2. This Declaration is being submitted in conjunction with an Amendment and Response to an Office Action having a mailing date of August 15, 2005.

3. The following discussion is provided in response to the Examiner's rejections of Claims 1, 6, 7, 24, 25, 28-31, 37, 38 and 43 under 35 U.S.C. § 102 in view of Sytkowski et al. (WO 99/02709) and further in response to the Examiner's rejections of Claim 32 or Claim 38 under 35 U.S.C. § 103 in view of Sytkowski et al. (WO 99/02709), alone or in combination with other references.

Although WO 99/02709 hypothecates direct EPO/IgG fusion proteins (*i.e.*, a fusion protein without an intervening linker), in fact, I submit that the only method described or referenced for producing such fusion proteins referenced by WO 99/02709 is inoperable for the production of direct EPO-IgG fusions. More particularly, on page 22, line 26, WO 99/02709 states that the contemplated EPO/IgG fusion proteins can be produced according to the methods of Steurer et al. (*J. Immunology* 155: 1165-1175, 1995), which uses a BamHI site to join cDNAs encoding CTLA4 and a mutant murine IgG2a-Fc domain (see page 1166, column 2, 2nd paragraph in Genetic Constructs section).

On page 24, line 20, WO 99/02709 teaches the following general method for constructing EPO fusion proteins : " The region of the Fcγ2a cDNA encoding the hinge, CH2 and CH3 domains of the heavy chain is then amplified by PCR using oligonucleotides designed to append unique *BamHI* and *XbaI* restriction sites onto the 5' and 3' ends[sic]...A cDNA encoding the erythropoietin is amplified by PCR using oligonucleotides designed to append unique *NotI* and *BamHI* restriction sites onto the 5' and 3' ends of this cDNA PCR respectively." This paragraph goes on to say that cDNAs encoding EPO and IgG-Fc fragment are ligated together and joined by the *BamHI* site. The application does not provide any additional methods for creating EPO/IgG fusion proteins, nor does the application provide any working example showing the actual fusion of EPO to an IgG domain.

However, WO 99/02709 clearly did not fully appreciate the structure of a direct fusion of EPO and IgG-Fc domains because it is impossible to use the method taught in WO 99/02709 (*i.e.*, using the method of Steurer et al.) to construct such a protein (*i.e.*, a *direct* fusion of EPO and an Fc domain. The amino acids at the end of EPO and the beginning of mouse or human IgG-Fc domains are such that they *cannot* be joined by a Bam III site (or any other restriction enzyme site that I am aware of) without *using a peptide linker* or *changing the amino acid sequences* of the proteins (thus effectively creating a synthetic peptide linker). Thus, WO 99/02709 is non-enabling for the construction of a direct fusion between EPO and an IgG Fc domain, as it is not possible to create such a protein using the teachings of this publication. Thus, I submit that WO 99/02709 did not reduce the invention to practice and have not actually taught an EPO-IgG fusion protein that is a direct fusion between EPO and IgG.

In contrast, I and my co-inventors provided a detailed method for constructing EPO/IgG fusion proteins in the present invention that do not contain a peptide linker (Example 4, pages 22 and 23), and we successfully used this method to construct such direct fusion proteins, which is shown in the working examples of the present application.

4. The following discussion is provided in response to the Examiner's rejections of Claims 15, 19, and 20 under 35 U.S.C. § 102 in view of Sytkowski (U.S. Patent No. 6,242,570).

Although the '570 patent hypothecates a direct fusion of EPO to EPO in column 3, line 32, there is no teaching anywhere in the '570 patent regarding how to produce such a protein, and no example of how to construct the EPO dimers without a linker are provided. The only multimeric fusion protein taught in the '570 patent is an EPO-EPO dimer joined by a peptide linker of 17 amino acids, and the linker is joined to the second EPO protein by a BamHI restriction site. Therefore, the only teaching in the '570 patent with regard to the production of an EPO multimeric protein again uses the introduction of BamHI sites as a means to join the proteins. For similar reasons as those discussed above in paragraph 3 with regard to EPO-Ig domain fusions, given the amino acid

sequences at the ends of the EPO proteins, it is not possible to create a *direct fusion* of EPO monomers (*e.g.*, an EPO dimeric protein) this way, because the *BamHI* site will always introduce additional amino acids that are not part of the EPO proteins, thus resulting in the creation of a linker between the monomers.

5. The following discussion is provided in response to the Examiner's rejections of Claims 2, 3-5, 26, 33, 42, 44, 45, 46, 52, 53, and 62-65 under 35 U.S.C. § 103 in view of Sytkowski et al. (WO 99/02709), alone or in combination with other references, including that of Curtis et al.

The Examiner contends that it would be obvious to use linkers of widely varying size and composition as generically mentioned in WO 99/02709 and Curtis et al., for example, because the use of linkers allegedly provides flexibility to a fusion protein. However, first, I submit that although WO 99/02709 postulates the production of EPO/IgG fusion proteins containing peptide linkers joining EPO and the IgG domains, they do not teach any amino acid sequences or DNA sequences of any such peptide linkers, and there are no actual working examples of the production of any EPO/Ig domain fusions in this publication.

I submit that it is not possible to predictably use any linker of any size or composition to reliably produce *biologically active* fusion proteins, particularly with regard to producing *biologically active* fusion proteins between large proteins such as cytokines, growth factors and immunoglobulin domains. Indeed, the motivation of providing flexibility, as the Examiner states in the Office Action, is insufficient to teach one skilled in the art how to produce biologically active fusion proteins using peptide linkers. Instead, I submit that the literature teaches that the size and sequence of peptide linkers can dramatically affect bioactivities of fusion proteins. Thus, without providing specific peptide amino acid sequences, or any other guidance regarding the selection and use of peptide linkers useful for the claimed proteins, all of which is missing from WO 99/02709 and Curtis et al., it is impossible to create any EPO/IgG fusion protein of a type envisioned by WO 99/02709 and predict whether or not it will have *in vitro* or *in vivo* biological activity, or whether the fusion protein will be biologically active at all. Moreover, I submit that the art in general does not suggest that linkers of the shorter size claimed in the present invention would be expected to produce biologically active fusions between cytokines, growth factors and immunoglobulin domains. I provide the following discussion and attached publications in support of my position.

Other publications available in the art at the time of the invention provide more specific teachings regarding the use of linkers in the creation of fusions between relatively large proteins (*e.g.*, proteins where secondary structures and tertiary structures must be considered). The literature indicates that specific activities of cytokine-growth factor/Ig fusion proteins vary depending upon the size of the peptide linker used to join the cytokine and Ig domain, and the specific amino acid

sequence of the peptide linker, and have generally taught that longer peptide linkers are preferred. These publications show that it would not have been obvious to one skilled in the art to produce the presently claimed fusion proteins that have the presently recited short linkers (including both the immunoglobulin fusion proteins and the multimeric fusion proteins), or to produce direct fusions between such proteins.

For example, Robinson et al. analyzes the role of linkers in a protein, ARC, in an effort to produce a single chain protein using a protein that naturally forms a dimer with itself (*i.e.*, a homodimer). Robinson et al. state on page 5930, col. 2, lines 1-7, that only linkers with 13 or more amino acids resulted in biologically active proteins. Linkers with 3, 8 or 9 amino acids were inactive in the fusion of Robinson et al. and linkers with 11 amino acids were only partially active. Thus, Robinson et al. teach away from using linkers of less than 13 (or even 11) amino acids for creating biologically active fusion proteins between large proteins. Based upon this reference, one skilled in the art would find it unpredictable whether biologically active EPO/Ig domain fusion proteins could be constructed using direct fusion or linkers between 2 and 7 amino acids, as has been exemplified by the present specification. In fact, I submit that the teachings of Robinson using other large proteins would dissuade one from trying to make direct fusions or use smaller peptide linkers. In contrast to Robinson et al., the present inventors have *demonstrated* the use of linkers of between 2 and 7 amino acids, to create a several different *biologically active* cytokine/growth factor fusions with Ig domains, as set forth in the present Examples, thus contradicting the findings of Robinson et al.

As another example, Qiu et al. (1998) reported that EPO-EPO fusion proteins joined by peptide linkers of 3-7 glycine residues have significantly reduced biological activities (4-10-fold) relative to wild type EPO, thus teaching away from using short linkers in such fusion proteins.

Chang (U.S. Patent No. 5,723,125) describe alpha interferon/IgG-Fc fusion proteins joined by a peptide linker. Chang found that an alpha interferon fusion protein containing a 16 amino acid linker (GGSGGSGGGGSGGGGS) had 5-10-fold greater specific activity in anti-viral assays than a related alpha interferon/IgG-Fc fusion protein containing a 6 amino acid linker (GGSGGS) (see column 5, lines 43-50). Similarly, in the present application (see Example 10), we found that alpha interferon /IgG fusion proteins containing a 7 amino acid peptide linker have approximately 100-fold reduced *in vitro* bioactivities relative to alpha interferon. A similar result was obtained when we constructed a beta interferon/IgG fusion protein containing a 7 amino acid linker. However, we demonstrated that the EPO-IgG fusion proteins containing the same 7 amino acid linker had *in vitro* bioactivities within 2- to 3- fold of EPO in *in vitro* bioassays (Example 3, page 20).

Therefore, the literature teaches that the length of the linker can dramatically impact the

biological activity of the resulting fusion protein, and further teaches that longer peptide linkers than those presently claimed were generally preferred at the time of the invention, in contrast to the teachings and examples provided by me and my coinventors.

6. I hereby declare that all statements made herein of my own are true and that all statements made on information and belief are believed to be true; and further that the statements were made with the knowledge that willful false statements and the like so made are punishable by fine or imprisonment, or both under Section 1001 of Title 18 of the United States Code, and that such willful false statements may jeopardize the validity of the subject application or any patent issuing therefrom.

Date: January 17, 2006 By: George N. Cox III

George N. Cox, III

Ex Vivo Coating of Islet Cell Allografts with Murine CTLA4/Fc Promotes Graft Tolerance[1]

Wolfgang Steurer,[2] Peter W. Nickerson,[2] Alan W. Steele,[3] Jurg Steiger, Xin Xiao Zheng, and Terry B. Strom[4]

Harvard Medical School, Department of Medicine, and Division of Immunology, Beth Israel Hospital, Boston, MA 02215

To test the hypothesis that blockade of B7-triggered costimulation by donor cells could preclude allograft rejection, we coated crude islet allograft preparations in vitro for 1 h with a murine CTLA4/Fc fusion protein. Murine CTLA4/Fc blocks the proliferative response in primary mixed lymphocyte cultures (MLC) and Con A-stimulated murine spleen cell cultures by 85 to 95%. Responder cells from a primary MLC containing mCTLA4/Fc were hyporesponsive upon restimulation to the same stimulator cells in a secondary MLC lacking mCTLA4/Fc. Because of mutations in the FcγRI and C1q binding sites of the Fc portion of the murine CTLA4/Fc fusion protein, the molecule binds to, but does not target, cells for Ab-dependent cellular cytotoxicity or complement-directed cytolysis. Although systemic immunosuppression was not applied, 42% (10 of 24) of B6AF1 recipients of islet allografts pretreated with CTLA4/Fc were permanently engrafted. Further, 50% of hosts bearing functioning islet allografts more than 150 days post-transplant were formally proved to be tolerant to donor tissues. A persistent $CD4^+$ and $CD8^+$ T cell infiltrate surrounding, but not invading, islet grafts in tolerant hosts was discerned. In control experiments, 89% (8 of 9) of islet allografts coated with mIgG3, and 100% ($n = 10$) pretreated with media alone were rejected. Thus, we conclude that 1) B7-triggered costimulation by donor APCs is an important element of rejection, and 2) blockade of the B7 pathway by in vitro allograft manipulation is able to induce tolerance. *The Journal of Immunology*, 1995, 155: 1165–1174.

T cells are central to the process of allograft rejection (1, 2). Activation of T cells bearing clonotypic receptors for donor alloantigen (alloAg)[5] is a two-step process in which occupancy of the TCR by alloAg provides the first, but not totally sufficient, signal for full activation (3, 4). Signal two ("costimulation") is derived from ligand-to-ligand interactions between the surfaces of APCs and T cells (reviewed in Ref. 5). The recently characterized members of the B7 "family" of proteins, expressed upon professional APCs, interact with CD28 and CTLA-4 T cell surface proteins and elicit unusually potent costimulatory signals (6–10). Of note, several groups have found that dendritic cells (DC) are the most potent professional APC in providing these costimulation signals to the naive T cell, whereas all professional APCs (i.e., DC, activated macrophages, or B cells) are able to stimulate primed T cells (11, 12). The unique capability of DCs to activate naive T cells may, in part, be related to their constitutive expression of B7 proteins (13). Moreover, naive T cells that recognize Ag in the absence of costimulatory second signals enter a long lived anergic state (i.e., fail to proliferate in response to antigenic rechallenge) (3) or undergo apoptosis (14).

Blockade of B7 to CD28/CTLA-4 interactions through the application of a soluble human CTLA4 fusion protein (hCTLA4Ig) powerfully inhibits T cell responses in vitro (8, 15). Furthermore, the systemic application of hCTLA4Ig to recipients of rodent allografts promotes engraftment, often leading to tolerance (16–18). In light of these findings, we have tested the hypothesis that coating intragraft $B7^+$ donor

Received for publication October 6, 1994. Accepted for publication May 18, 1995.

The costs of publication of this article were defrayed in part by the payment of page charges. This article must therefore be hereby marked *advertisement* in accordance with 18 U.S.C. Section 1734 solely to indicate this fact.

[1] This work supported by grants from the FWF Austrian Science Foundation (W.S.), the Medical Research Council of Canada (P.W.N.), the Swiss National Foundation (J.S.), the American Heart Association and the National Kidney Foundation of America (A.W.S.), and the National Institutes of Health (T.B.S.).

W. Steurer and P. W. Nickerson were equal contributors to the work in this article.

[3] Current address: Dr. Alan W. Steele, Division of Renal Medicine, University of Massachusetts Medical Center, Worcester, MA 01655.

[4] Address correspondence and reprint requests to Dr. Terry Strom, Department of Medicine, and Division of Immunology, Beth Israel Hospital, 330 Brookline Avenue, Boston, MA 02215.

[5] Abbreviations used in this paper: alloAg, alloantigen; DC, dendritic cell; hCTLA4Ig, human CTLA4 IgG fusion protein; (I) or (NI) mCTLA4/Fc, lytic or nonlytic murine CTLA4/Fcγ2a heavy chain chimeric fusion molecule; ADCC, antibody dependent cellular cytotoxicity; CDC, complement-directed cytolysis; MST, mean survival time.

0022-1767/95/$02.00

cells ex vivo, before transplantation, would preclude CD28/CTLA-4 costimulatory signals and enhance the potential for long-term engraftment and tolerance. For this purpose, we designed a nonlytic (NL) murine CTLA4/Fcγ2a heavy chain (mCTLA4/Fc) chimeric fusion molecule. Because of mutations in the FcγRI and C'1q binding sites of the Fcγ2a portion of the fusion protein, the molecule binds to, but does not target, APCs for lysis through Ab-dependent cellular cytotoxicity (ADCC) or complement-directed cytolysis (CDC) (i.e., mCTLA4/Fc is a competitive blocker for occupation of B7 proteins). Unlike the experiments in which hCTLA4Ig was systemically administered to the recipient (16–18), our strategy of coating the graft with mCTLA4/Fc ex vivo should only block costimulation associated with donor graft Ags, as we do not apply systemic immunosuppression. In this report we describe the characterization of (NL) mCTLA4/Fc in vitro and its potential to induce in vivo graft-specific tolerance following ex vivo treatment of murine islet cell allografts.

Materials and Methods

Animals

Six- to eight-week-old male B6AF1, DBA/2J, C57BL/6, and A.SW mice were obtained from The Jackson Laboratory (Bar Harbor, ME) and housed under standard conditions both before and after transplantation.

Monoclonal Abs

The following mAbs were used: rat anti-mouse IgG2a (PharMingen, San Diego, CA), rat anti-mouse IgG2a-horseradish peroxidase (PharMingen), FITC-labeled goat anti-mouse IgG (Sigma Chemical Co., St. Louis, MO), rat anti-mouse CD4 and rat anti-mouse CD8 (PharMingen), biotinylated rabbit anti-rat mAb (Vector, Burlingame, CA), hamster anti-mouse B7-1 16-10 A1 (a gift of Dr. H. Reiser, Dana-Farber Cancer Institute, Boston, MA), FITC-rabbit anti-hamster IgG (Pierce, Rockford, IL), and mouse IgG2a (κ) and IgG3 (κ) hybridoma proteins (Cappel, West Chester, PA).

Cell lines

The following cell lines were used: murine IgG2a-secreting hybridoma 116-13.1 (American Type Culture Collection (ATCC), Rockville, MD), CHO-K1 (ATCC), CHO cells transfected with human FcγRI cDNA (a gift of Dr. B. Seed, Massachusetts General Hospital, Boston, MA), and CHO cells transfected with mouse B7-1 and CHO cells transfected with vector alone (gifts of Dr. H. Reiser, Dana-Farber Cancer Institute, Boston, MA).

Cell culture

Cell culture reagents, unless otherwise stated, were obtained from Life Technologies, Inc. (Grand Island, NY). Cells were grown in complete RPMI 1640, i.e., RPMI supplemented with L-glutamine, 10% heat-inactivated FCS, 10 mM HEPES, 0.1 mM nonessential amino acids, 1 mM sodium pyruvate; 5×10^{-5} M 2-ME (Sigma Chemical Co.); 100 U/ml penicillin, and 100 μg/ml streptomycin. CHO-K1 transfectants were maintained in DMEM with 5% FCS, 100 U/ml penicillin, and 100 mg/ml streptomycin. Transfected cell lines were cultured in Ultraculture (BioWhittaker, Walkersville, MD) serum-free media supplemented with L-glutamine, penicillin, and streptomycin.

Plasmids

The murine CTLA-4 cDNA plasmid F41F4 was a generous gift from Dr. P. Golstein, Centre d'Immunologie, INSERM-CNRS de Marseille Luminy, France (19). The eukaryotic expression vector Rc/CMV (Invitrogen, San Diego, CA) was modified by deletion of all three *Bam*H I sites and its unique *Apa*I site. The PCR II vector (Invitrogen) was used for TA cloning of cDNA amplified by the PCR.

Genetic constructs

Total RNA was purified, on a cesium chloride (Life Technologies, Inc.) gradient, from the murine IgG2a-secreting hybridoma 116-13.1 and then reverse transcribed to cDNA using oligo-dT_{12-18} (Pharmacia, Piscataway, NJ) primers and M-MLV reverse transcriptase (Life Technologies, Inc.). The region of the Fcγ2a cDNA encoding the hinge, CH2, and CH3 domains of the heavy chain was then amplified by PCR using oligonucleotides designed to append unique *Bam*HI and *Xba*I restriction sites onto the 5′ and 3′ ends of the Fcγ2a cDNA fragment respectively. This cDNA PCR product was digested with *Bam*HI and *Xba*I restriction enzymes (New England Biolabs, Beverly, MA) and gel purified in preparation for ligation (see below).

A 503-bp cDNA fragment of the murine CTLA-4 cDNA plasmid F41F4, encoding the sequence for the leader and extracellular domains of CTLA-4, was amplified by PCR using oligonucleotides designed to append unique *Not*I and *Bam*HI restriction sites onto the 5′ and 3′ ends of this cDNA, respectively. The cDNA was then cloned into the PCR II vector, excised using *Not*I (New England Biolabs) and *Bam*HI restriction endonucleases, and gel purified. Subsequently, the CTLA-4 cDNA, the previously prepared Fcγ2a cDNA, and the cDNA of the modified Rc/CMV vector opened at the cloning site with *Not*I and *Xba*I restriction endonucleases were mixed and ligated using T4 DNA ligase (Life Technologies, Inc.). The correct reading frame at the junction of the CTLA-4 to Fc cDNAs was confirmed by DNA sequencing.

PCR-assisted, site-directed mutagenesis of the Fcγ2a cassette was used to render nonfunctional (a) the high affinity FcγRI receptor binding site by substituting Glu for Leu 235 (20), and (b) the C'1q binding site by substituting Glu 318, Lys 320, Lys 322 with Ala residues (21). The cDNA mutations were confirmed by DNA sequencing. Subsequent expression of these two CTLA-4/Fc constructs results in murine CTLA4/Fc fusion proteins with or without ADCC and CDC activity, respectively (i.e., lytic (L) or (NL) mCTLA4/Fc; see *Results*).

mCTLA4/Fc expression and purification

To achieve stable expression, 20 μg of the murine CTLA4/Fc plasmid construct was linearized by *Pvu*I digestion (New England Biolabs) and electroporated into 10^7 CHO-K1 cells. Transformed CHO-K1 cells were selected with 1 mg/ml G418 (Life Technologies, Inc.) and subsequently cloned by limiting dilution. Established cell lines were then screened for mCTLA4/Fc production by an ELISA specific for murine IgG2a. High producing clones were cultured in serum-free media for 12 days. Supernatant was size (0.2 μm pore) filtered, and Tris, pH 8.0, was added to a final concentration of 50 mM, and then passed over a protein A-Sepharose column (Pharmacia) equilibrated with 0.05 M Tris-buffered saline pH 8.0, and eluted with 0.04 M sodium citrate, pH 4.5. Eluted fractions were immediately buffered to a pH of 7.4 by addition of one-tenth vol of 1 M Tris, pH 8.0. Fractions with greatest absorbance at 280 nm were then pooled and dialyzed against PBS overnight at 4°C.

In vitro characterization of (L) and (NL) mCTLA4/Fc

Confirmation of size and isotype specificity. Affinity-purified proteins were characterized by Laemmeli gel electrophoresis under reducing (+DTT) and nonreducing (−DTT) conditions. After transfer to a nylon membrane (Immobilon-P, Millipore, Bedford, MA) the protein was, 1) visualized by Coomassie blue staining, and 2) analyzed by Western blot to confirm the IgG2a isotype specificity using a rat anti-mouse IgG2a as the primary Ab, a biotinylated rabbit anti-rat mAb as the secondary Ab, and visualized with avidin-HPRO complex (Vector) using 3′,3′-diaminobenzidine (DAB; Vector) for detection of enzyme activity.

Confirmation of B7-1 binding. CHO-B7-1 transfected cells (2.5×10^5) were incubated with saturating concentrations (10 μg/ml) of (L) or (NL) mCTLA4/Fc or 10 μg/ml of mIgG2a (negative control) at 4°C, washed twice, and reincubated with a 1:125 dilution of FITC-conjugated goat anti-mouse IgG mAb. To confirm the B7-1 surface expression of the transfected CHO cells (positive control), the cells were incubated with saturating concentrations (100 μg/ml) of hamster anti mouse B7-1 mAb

at 4°C, washed twice, and reincubated with a 1:60 diluted FITC-rabbit anti-hamster Ab. Subsequently the cells were fixed in 1% formaldehyde (Sigma Chemical Co.) and analyzed on a FACStar^{Plus} (Becton Dickinson, Franklin Lakes, NJ).

Assessment of FcγRI binding. CHO-FcγRI-transfected cells (2.5×10^5) were incubated with saturating concentrations (10 μg/ml) of (L) or (NL) mCTLA4/Fc or 10 μg/ml of mIgG2a (positive control) at 4°C, washed twice, and reincubated with a 1:125 dilution of FITC-conjugated goat anti-mouse IgG mAb. Cells incubated with media alone, and then incubated with a 1:125 dilution of FITC-conjugated goat anti-mouse IgG mAb served as a negative control. Subsequently cells were fixed in 1% formaldehyde and analyzed on a FACStar^{Plus}.

Complement-directed cytotoxicity assay. CHO-B7-1-transfected cells (10^6) were labeled with 100 μCi ^{51}Cr (Dupont NEN, Boston, MA), washed three times, and distributed in a density of 10^4 cells/well in flat bottom microtiter plates followed by a 45-min incubation with various dilutions of (L) or (NL) mCTLA4/Fc and rabbit low tox complement (Cedarlane, Hornby, Ontario, Canada) in a dilution of 1:10 at 37°C. The ^{51}Cr released into 100 μl of the culture supernatant was measured in a gamma counter (Packard, Downers Grove, IL). Maximum ^{51}Cr release was determined by disruption of ^{51}Cr-labeled targets through Nonidet P-40 lysis. The percent specific lysis was calculated according to the formula:

% specific lysis = (experimental cpm − background cpm)/

(total release cpm − background cpm) × 100.

All experiments were performed in triplicate.

Assessment of antiproliferative activity. 1) Con A activation of unfractionated spleen cells: B6AF1 spleen cells were prepared by mincing the spleen between two glass slides. After washing, RBCs were lysed by exposure to tris ammonium chloride buffer for 5 min at room temperature; the mixture was then washed. Viability, determined by trypan blue (Life Technologies, Inc.) staining, exceeded 90%. Following incubation with (L) mCTLA4/Fc or control mIgG2a mAb in 1:4 serial dilutions for 1 h, 3×10^5 spleen cells were cultured in flat bottom 96-well microtiter plates in quadruplicate samples for 48 h in a final volume of 200 μl. Proliferation was estimated by pulsing the cultures for 6 h before termination with 1 μCi/well [^{3}H]thymidine (Dupont NEN), and [^{3}H]thymidine incorporation was measured using a liquid scintillation counter (Beckmann LS 2800, Palo Alto, CA). 2) MLC: 10^5 DBA2/J ($H\text{-}2^d$) responder cells were preincubated in serial dilutions of (L) mCTLA4/Fc (see above) for 1 h at 37°C in round bottom 96-well microtiter plates. Subsequently irradiated (3000 rad) C57BL/6 ($H\text{-}2^b$) stimulator cells were added at a ratio of 2:1, and the cultures were pulsed with 1 μCi/well [^{3}H]thymidine and harvested on day 5. Thymidine incorporation was measured using a liquid scintillation counter. For restimulation assays, MLCs were established, as above, using 2×10^7 spleen cells at a 1:1 responder:stimulator ratio in a 6-well culture plate. Cells were washed extensively on day 7, cultured for another 3 days in medium without mCTLA4/Fc or mIgG2a, and then restimulated with irradiated C57BL/6 spleen cells. In some restimulation experiments rIL-2 (50 U/ml; Hoffmann-La Roche, Nutley, NJ) was added to MLCs containing cells previously exposed to mCTLA4/Fc to determine whether the cells were anergic. Cultures were then pulsed with 1 μCi/well [^{3}H]thymidine, and aliquots were harvested daily on days 1 through 7. Determination of [^{3}H]thymidine incorporation was measured as above.

Islet cell allograft pretreatment with (NL) CTLA4/Fc

Crude islet cell isolates were harvested from DBA/2J mice by collagenase digestion and Ficoll density gradient separation as previously described (22). Approximately 400 to 600 islets per transplant were incubated for 1 h with either media alone, control protein (mIgG3; 10 μg/ml), or 10 μg/ml (NL) mCTLA4/Fc in RPMI at 37°C. A 200-μl pipette was prepared with a gel foam plug in the tip. The crude islet cell preparation contained in a volume of 200 μl (i.e., 2 μg of mIgG3 or (NL) CTLA4/Fc) is then placed into the pipette on top of the plug and pelleted by centrifugation. Excess media (ca. 195 μl) is removed to greatly diminish the carry over of unbound (NL) CTLA4/Fc into the circulation of the recipient. Another gel foam plug was placed in the tip above the pellet. The virtually solid pellet of islets (volume ~5 μl), is then injected under the left renal capsule of B6AF1 recipients rendered diabetic 7 days previously by a single 225 mg/kg i.p. injection of streptozotocin (Sigma Chemical Co.). Recipients received no systemic immunosuppression. In another experimental group ($n = 8$), the grafts were not manipulated ex vivo; however, the recipients received a single 50-μg i.p. dose of (NL) mCTLA4/Fc immediately post-transplantation. Graft function was monitored by tail blood glucose measurements using the Chemstrip bG and Accu-Chek III blood glucose monitor system (Boehringer Mannheim, Indianapolis, IN). Post-transplant, primary graft function was defined as a blood glucose level <11.1 mmol/l, and subsequent graft failure defined by consistent blood glucose levels >16.5 mmol/l. The method of Litchfield was used to determine statistically significant differences in graft survival curves, i.e., $p < 0.05$ (23).

To detect graft tolerance, animals with functioning grafts were challenged >150 days post-transplantation with an i.p. injection of 5×10^7 irradiated (3000 rad) donor splenocytes (24). To determine whether tolerance was donor alloAg-specific, mice remaining euglycemic after donor splenocyte challenge underwent unilateral nephrectomy to remove the islet graft. Post-nephrectomy, the blood glucose levels were followed to document the occurrence of hyperglycemia as a criterion for graft removal. These mice were then divided into two experimental groups and transplanted with either an islet graft from the original donor strain (DBA/2J) or islets from a third party donor (A.SW).

Immunohistochemistry

The left kidney containing the islet cell graft of a tolerant animal (i.e., the graft was functioning day 200 post-transplantation and day 50 post donor spleen cell challenge) was removed and embedded in OCT compound (Miles, Elkhart, IN). Serial frozen sections were either fixed in cold acetone for immunocytochemistry or fixed in methanol for hematoxylin-eosin staining. Immunohistology was performed according to a protocol described by Bogen, Fogelman, and Abbas (25). Briefly, 0.3-μm sections were sequentially blocked with mouse serum, avidin, biotin; quenched with H_2O_2; and then incubated with rat anti-mouse CD4 or CD8 mAbs for 45 min in 0.05 M Tris buffer (pH 7.6) at room temperature. Ab binding was detected with a biotinylated rabbit anti-rat mAb and avidin-horseradish peroxidase complex, using 3',3'-diaminobenzidine for detection of enzyme activity. Negative controls were processed as above with the exclusion of the primary Ab. Sections were counter stained with methyl green (Sigma Chemical Co.).

Results

CTLA-4, a counter receptor for the B7 family of proteins, is expressed on activated T cells and binds with a 20-fold greater affinity to B7-1 than CD28 (8). Soluble hCTLA4Ig effectively blocks the cognate interaction of B7 and cell-bound CD28 or CTLA-4 (8). We have constructed a soluble homodimeric fusion protein consisting of the extracellular segment of murine CTLA-4 and the murine Fcγ2a heavy chain. The cDNA sequence encoding the 5'-untranslated, leader and extracellular exons of mCTLA-4 was ligated to the cDNA sequence encoding the hinge, CH2, and CH3 of the mIgG2a heavy chain that had previously been cloned into a modified eukaryotic expression vector Rc/CMV. The (L) and (NL) mCTLA4/Fc constructs were expressed in CHO-K1 cells, and the proteins purified from serum-free culture supernatant by passage over protein A-Sepharose columns. The protein A adherent fraction was applied to a SDS-polyacrylamide gel under reducing conditions (+DTT), and Coomassie blue staining showed a single protein band at the expected molecular size of ~55 kDa (Fig. 1, *lanes a* and *b*). The murine IgG2a and mIgG3 control proteins migrated as two protein bands of 25 and 50 kDa, reflecting the κ light chain and IgG2a heavy chain (Fig. 1, *lanes c* and *d*). Under nonreducing conditions (−DTT), (L), and (NL) mCTLA4/Fc

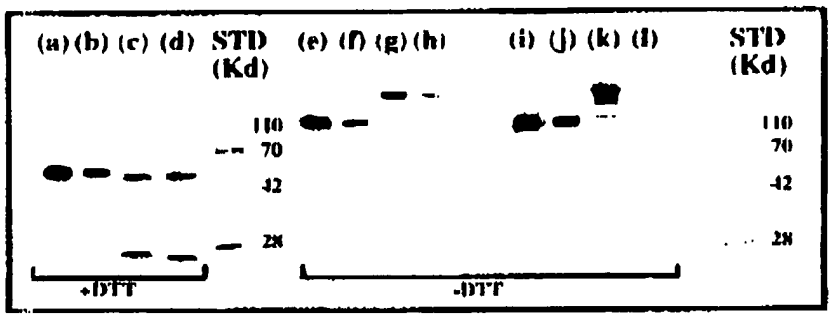

FIGURE 1. Confirmation of size and isotype specificity of (L) and (NL) mCTLA4/Fc. Affinity-purified protein was characterized by Laemmeli gel electrophoresis under reducing (+DTT) and nonreducing (−DTT) conditions: 1) visualized by Coomassie blue staining (*lanes a* to *h*) or 2) stained with rat anti mouse IgG2a by Western blot to confirm the IgG2a isotype specificity (*lanes i* to *l*). (L) CTLA4/Fc: *lanes a, e, i*; (NL) CTLA4/Fc: *lanes b, f, j*; mIgG2a: *lanes c, g, k*; mIgG1: *lanes d, h, l*. Blots were scanned using Scanjet II software (Hewlett Packard, Greeley, CO).

run as a single bands with a molecular size of ~110 kDa, consistent with the formation of homodimers (Fig. 1, *lanes e* and *f*). The specific binding of a rat anti-mouse IgG2a mAb to mCTLA4/Fc (Fig. 1, *lanes i* and *j*) confirmed the isotype specificity of the Fc portion of the fusion proteins.

The capacity of (L) or (NL) mCTLA4/Fc to stain CHO cells transfected with the full length mouse B7–1 cDNA was analyzed. These cells express high levels of mouse B7–1 as assessed by staining with anti-mB7–1 mAb 16-10 A1 and detection by FACS analysis (Fig. 2, *panel D*). CHO-B7–1 cells were incubated with (L) or (NL) mCTLA4/Fc or control mIgG2a at saturating concentrations. B7-negative CHO cells, transfected with vector alone, served as a negative control in the same experiment (Fig. 2, *panels A, C, E, G*). (L) and (NL) mCTLA4/Fc bind to CHO-B7–1 cells, as demonstrated by the shift in FACS profiles (Fig. 2, *panels F* and *H*), whereas CHO-mock cells were not bound by (L) or (NL) mCTLA4/Fc (Fig. 2, *panels E* and *G*). The isotype control (mIgG2a) did not bind to either the CHO-mock or B7–1$^+$ CHO cells (Fig. 2, *panels A* and *B*).

The Fc portion of murine IgG2a is bound by leukocytes expressing the high affinity FcγRI receptor (26). Therefore, certain FcγRI$^+$ leukocytes can effect ADCC against Ab-bound cells. Furthermore, the murine IgG2a isotype efficiently binds C1q to initiate CDC against Ab-bound cells (26). To block costimulation rather than targeting CTLA4/Fc-bound cells for lysis, we mutated the high affinity FcγRI binding site and the C1q binding site of Fcγ2a to create a mCTLA4/Fc fusion protein that will bind to the B7 family of proteins but be devoid of ADCC or CDC activity ((NL) mCTLA4/Fc).

The FcγRI binding site on Fcγ2a is located in the CH2 domain of the Fc fragment. Following the report by Duncan et al. (20), Leu 235 was mutated to Glu by PCR-assisted, site directed mutagenesis. To determine whether the single amino acid mutation diminished the high affinity FcγRI receptor binding function of mCTLA4/Fc, we as-

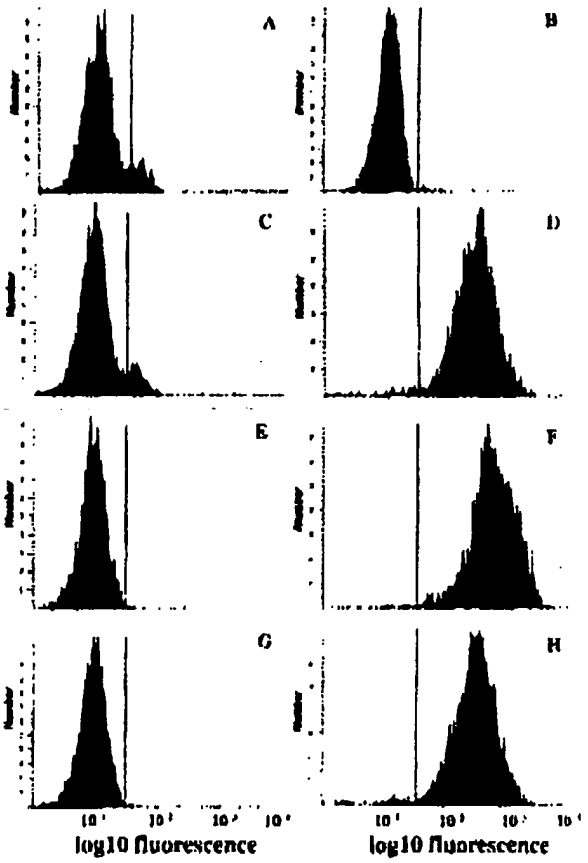

FIGURE 2. Confirmation of B7–1 binding by (L) and (NL) mCTLA4/Fc. CHO cells transfected with vector alone (*panels A, C, E,* and *G*) or CHO-B7–1-transfected cells (2.5×10^5) were incubated with 10 μg/ml of mIgG2a (negative control; *panels A* and *B*), 100 μg/ml of an anti-B7–1 mAb (positive control; *panels C* and *D*), 10 μg/ml (L) mCTLA4/Fc (*panels E* and *F*), or 10 μg/ml of (NL) mCTLA4/Fc (*panels G* and *H*).

sessed the binding activities of (NL) and (L) mCTLA4/Fc to CHO-FcγRI-transfected cells by FACS analysis. (L) CTLA4/Fc i.e., carrying the wild-type Fcγ2a sequence, readily bound to CHO-FcγRI-transfected cells (Fig. 3, *panel B*, open profile). In contrast, the (NL) mCTLA4/Fc, carrying the mutated Fcγ2a sequence, exhibited a dramatic reduction in binding to CHO-FcγRI-transfected cells (Fig. 3, *panel B*, solid profile). Murine IgG2a, which bound to FcγRI$^+$ target cells in a similar manner as (L) mCTLA4/Fc, served as a positive control (Fig. 3, *panel A*, open profile).

We next studied the capacity of (L) or (NL) mCTLA4/Fc proteins to direct complement-dependent lysis of B7− $^+$ target cells. In addition to the single amino acid mutation (Leu 235 to Glu) in the CH2 Fcγ2a domain of the (NL) molecule, three closely adjacent amino acids at positions Glu 318, Lys 320, and Lys 322 were replaced by alanine residues in the (NL) CTLA4/Fc molecule. Glu 318, Lys 320, and Lys 322 are highly conserved throughout the evolution of IgGs, and mutations to alanine at these sites are known to reduce C'1q binding by 100-fold (21). CHO-B7-1 transfectants were labeled with ^{51}Cr and incubated with (L) mCTLA4/Fc, (NL) mCTLA4/Fc, mIgG2a, or mIgG3 (negative controls) and a 1:10 dilution of rabbit low tox complement. After 45 min, lysis of CHO-B7-1 cells was assessed by quantitation of the ^{51}Cr released into the supernatant. In the presence of C' + (L) mCTLA4/Fc, 20 to 21% specific lysis of CHO-B7-1 cells was detected (Fig. 4). The presence of C' + (NL) mCTLA4/Fc induced only a 1% specific lysis of CHO-B7-1 cells (Fig. 4). Complement alone, or mIgG2a + C', or mIgG3 + C', was ineffective in directing B7-1$^+$ target cell lysis (Fig. 4).

To ascertain whether the mCTLA4/Fc fusion molecule is able to block murine T cell activation, we examined the effect of CTLA4/Fc in two in vitro systems of T cell activation. First, the in vitro immunosuppressive potential of mCTLA4/Fc was tested in a Con A-driven proliferation system in which APCs provide important costimulatory signals (27). The blockade of B7 sites with (L) mCTLA4/Fc (Fig. 5, *panel A*), (NL) mCTLA4/Fc (data not shown), but not control IgG2a, proteins produced a dose-dependent antiproliferative effect. Next, we tested the effect of (L) mCTLA4/Fc on allogeneic MLCs. Proliferation, as estimated by [^{3}H]thymidine incorporation on day 5 of culture, was markedly inhibited by (L) mCTLA4/Fc (Fig. 5, *panel B*). On a per dose basis, the MLR was more sensitive to the inhibitory effects of mCTLA4/Fc than Con A cultures.

Previous studies have shown that interference with the CD28 pathway during T cell priming results in Ag-specific hyporesponsiveness upon secondary restimulation (15). To test whether mCTLA4/Fc exerts similar long lasting effects on secondary murine T cell responses, DBA2/J (H-2^d) spleen cells were cultured with irradiated C57Bl/6 (H-2^b) spleen cells for 7 days in medium containing 10 μg/ml mCTLA4/Fc or control mIgG2a. Cells were then washed to remove CTLA4/Fc or IgG and rested for an additional 3 days in fresh medium before restimulation with original (H-2^b) stimulator spleen cells in the absence of mCTLA4/Fc. Cells primed in the presence of control IgG2a proliferated in a second set fashion upon restimulation with the original stimulator cells and reached maximum [^{3}H]TdR incorporation on days 2 to 3 (Fig. 6, *panel A*). In contrast, responder cells (DBA/2J) primed in the presence of mCTLA4/Fc did not proliferate in response to reconfrontation with the original C57Bl/6 strain stimulator cells (i.e., proliferation did not exceed 10% of the maximum proliferation of the positive control cultures at any time point) unless rIL-2 was added to the system (Fig. 6, *panel B*).

As documented by Gotoh et al., crude islet preparations contain islets, vascular tissue, ductal fragments, and lymph nodes (ca. 30 to 40 lymph nodes per graft preparation)

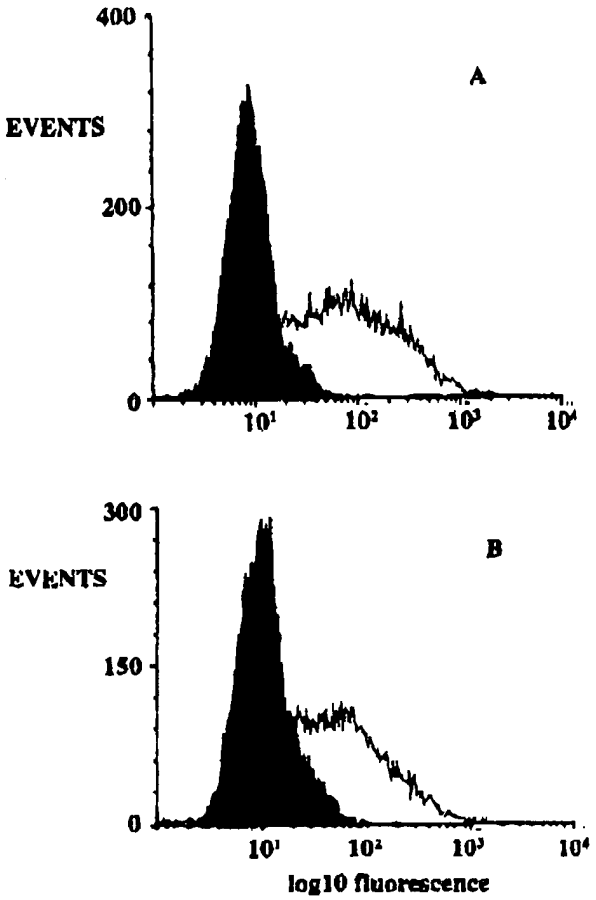

FIGURE 3. (L) but not (NL) mCTLA4/Fc binds the high affinity FcγRI. *A*, CHO-FcγRI-transfected cells (2.5×10^5) were incubated with 10 μg/ml of mIgG2a (positive control, open profile) or media alone (negative control, solid profile). *B*, CHO-FcγRI-transfected cells were incubated with 10 μg/ml of (L) mCTLA4/Fc (open profile) or (NL) mCTLA4/Fc (solid profile).

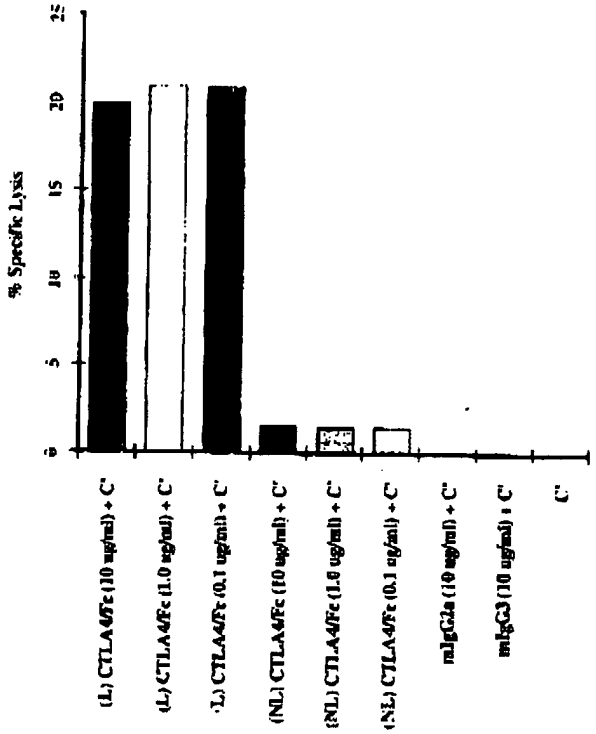

FIGURE 4. (L) but not (NL) mCTLA4/Fc lyses cells expressing B7-1. CHO B7-1-transfected cells (10^6) labeled with 100 μCi ^{51}Cr were incubated with various concentrations of (L) or (NL) mCTLA4/Fc and rabbit low tox complement (see *Materials and Methods*). Cells incubated with mIgG2a + C', mIgG3 + C' or C' alone served to define nonspecific lysis.

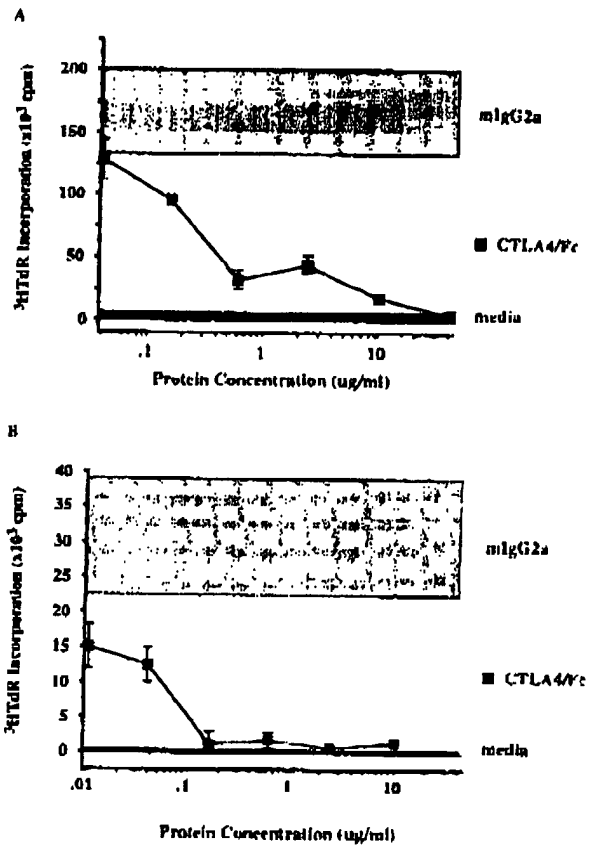

FIGURE 5. mCTLA4/Fc inhibits the proliferation of unfractionated spleen cells cultures. *A*, Con A stimulated B6AF1 spleen cells were incubated with varying concentrations of (L) mCTLA4/Fc, control mIgG2a mAb, or media alone. *B*, In a MLC, aliquots of DBA2/J ($H\text{-}2^d$) responder cells (10^5 cells/well) preincubated with serial dilutions of (L) mCTLA4/Fc were stimulated with irradiated (3000 rad) C57Bl/6 ($H\text{-}2^b$) spleen cells (2×10^5 cells/well) and harvested on day 5 of culture.

(22). Indeed we have used the same methods of islet preparation and the same strain combinations as studied in the report of Gorczynski et al. (23). In considering the forgoing, we hypothesized that (NL) mCTLA4/Fc could be incubated with islet grafts in vitro, before transplantation, to block B7-mediated costimulation by donor tissues in the belief that lymph node cells (other than islet cells) provide B7-mediated costimulatory signals. All islet grafts (n = 24) pretreated with (NL) mCTLA4/Fc demonstrated primary graft function by day 6 post-transplantation. Of these, 10 (42%) went on to long-term engraftment (i.e., >150 days) (Fig. 7). In control experiments, islets were precultured with mIgG3. Murine IgG3 proteins do not engage murine FcγRI and weakly activate C' compared with mIgG2a isotypes (28). Moreover, IgG Igs only effect efficient CDC activity as a multimeric complex whereas monomeric IgG can bind FcRs (26). Therefore, a monoclonal mIgG3, which does not bind B7, was chosen as a control ligand for the (NL) mCTLA4/Fc fusion protein. All of IgG3-treated islet grafts (n = 9) demonstrated primary graft function, and 89% were acutely rejected (Fig. 7). Islets that were cultured in medium alone (n = 10) showed primary function and were acutely rejected by day 44 (Fig. 7). Hence, the short incubation period of 1 h of islet graft pretreatment did not lead to significant engraftment unless (NL) CTLA4/Fc was present. Moreover, 88% of islet grafts placed into recipients treated with a single 50-μg i.p dose of (NL) CTLA4/Fc immediately post-transplant were rejected. Hence, the effect of ex vivo coating of the islet graft with (NL) CTLA4/Fc was not likely because of a carry over of (NL) CTLA4/Fc into the circulation of the recipient, insofar as the (NL) CTLA4/Fc-coated crude islet cell preparation could at most bear 2 μg of (NL) CTLA4/Fc. Indeed, it is likely that even less (NL) CTLA4/Fc was bound to the crude islet cell preparations.

To determine whether graft tolerance was achieved through coating of donor tissue with (NL) CTLA4/Fc, hosts bearing long-term functioning islet grafts (i.e., >150

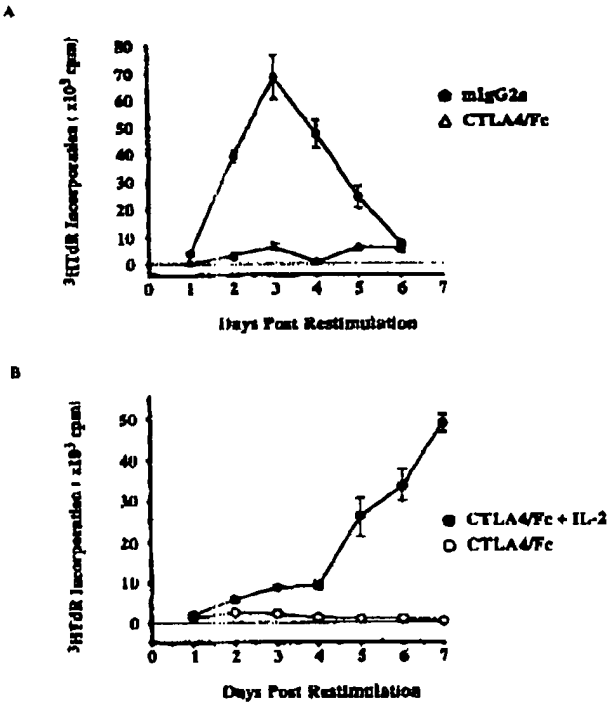

FIGURE 6. mCTLA4/Fc induces hyporesponsiveness upon restimulation of an MLC with donor Ag. *A*, MLCs were established using 2×10^7 spleen cells at a 1:1 responder:stimulator ratio in 6-well culture plates in the presence of 10 μg/ml mCTLA4/Fc or mIgG2a. Cells were washed extensively on day 7, cultured for another 3 days in medium without mCTLA4/Fc or mIgG2a, and then restimulated with irradiated C57BL/6 spleen cells. Aliquots were harvested daily on days 1 through 7. *B*, Hyporesponsive cells were cultured with or without the addition of rIL-2 (50 U/ml) during restimulation with irradiated C57BL/6 spleen cells.

days) were challenged with 5×10^7 irradiated donor spleen cells; donor spleen cells have been previously documented to provide a very strong donor Ag challenge (24). Interestingly, 50% (5 of 10) of these recipients failed to reject their grafts. To test for the presence of donor-specific tolerance, four mice remaining euglycemic after spleen cell challenge underwent unilateral nephrectomy to remove the islet graft. All nephrectomized mice (4 of 4) developed hyperglycemia, indicating that euglycemia had been dependent on the presence of the graft and not endogenous insulin secretion. The two mice receiving third party islet grafts (A.SW, H-2^u) and the two mice receiving original donor strain islet grafts (DBA/2J, H-2^d) normalized their blood sugars, indicating primary graft function. While recipients of DBA/2J strain grafts continued to maintain euglycemia >90 days post-transplant, the recipients of third party grafts became hyperglycemic on day 12 post-transplant.

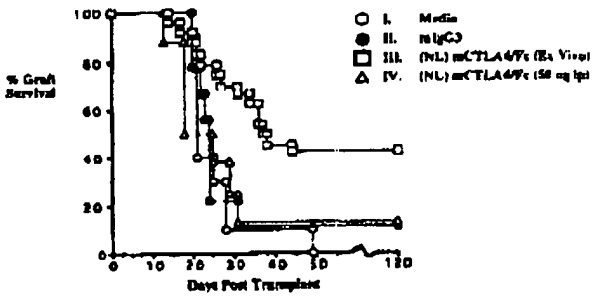

FIGURE 7. Islet cell allograft pretreatment with (NL) CTLA4/Fc prolongs engraftment. Crude islet cell isolates harvested from DBA/2J mice were incubated for 1 h before the implantation with either media alone (group I, $n = 10$), 10 μg/ml mIgG3 (group II, $n = 9$), or 10 μg/ml (NL) mCTLA4/Fc (group III, $n = 24$). Group IV, $n = 8$ was treated with a single i.p. dose of 50 μg (NL) mCTLA4/Fc on the day of transplantation. The significance level of graft survival between the four groups are: $p < 0.05$ for I, II, or IV vs III, $p > 0.05$ for I vs II or IV, and II vs IV.

Histologic analysis of islet cell allografts harvested from tolerant animals (i.e., >day 150 post-transplantation and >day 50 post donor spleen cell challenge) demonstrated a dense mononuclear cell infiltrate surrounding, but not invading, the islets (Fig. 8). The majority of these cells were $CD4^+$ cells; a significant number of $CD8^+$ cells (approximately 30% the level of $CD4^+$ cells) were also detected.

Discussion

To aid the study of the biologic role of the murine B7-CD28 costimulatory pathway, we have designed, expressed, and purified soluble murine CTLA4/Fcγ2a fusion molecules (Fig. 1). Recently, Finck, Linsley, and Wofsy have also developed a murine CTLA4/Fcγ2a fusion protein (29). Compared with human-based fusion proteins, the murine fusion molecule should be less immunogenic in murine models. These mCTLA4/Fc fusion molecules, as expected, bind to the murine B7 proteins (Fig. 2). Indeed, mCTLA4/Fc is a potent inhibitor of in vitro T cell responses. In primary murine MLC or Con A-stimulated spleen cell cultures, mCTLA4/Fc blocks the proliferative response by 85 to 95% (Fig. 5). That the action of mCTLA4/Fc was, in fact, mediated by blocking CD28 signal transduction rather than blocking APC/T cell adhesion is supported by the fact that addition of Con A still results in typical cell clustering after incubation of spleen cells with mCTLA4/Fc (our unpublished observation). As noted with hCTLA4Ig (15) in a human MLC system, responder cells from a primary murine MLC containing mCTLA4/Fc were hyporesponsive upon restimulation to the same stimulator cells in a secondary MLC lacking mCTLA4/Fc unless rIL-2 was added to the system (Fig. 6). Thus, both

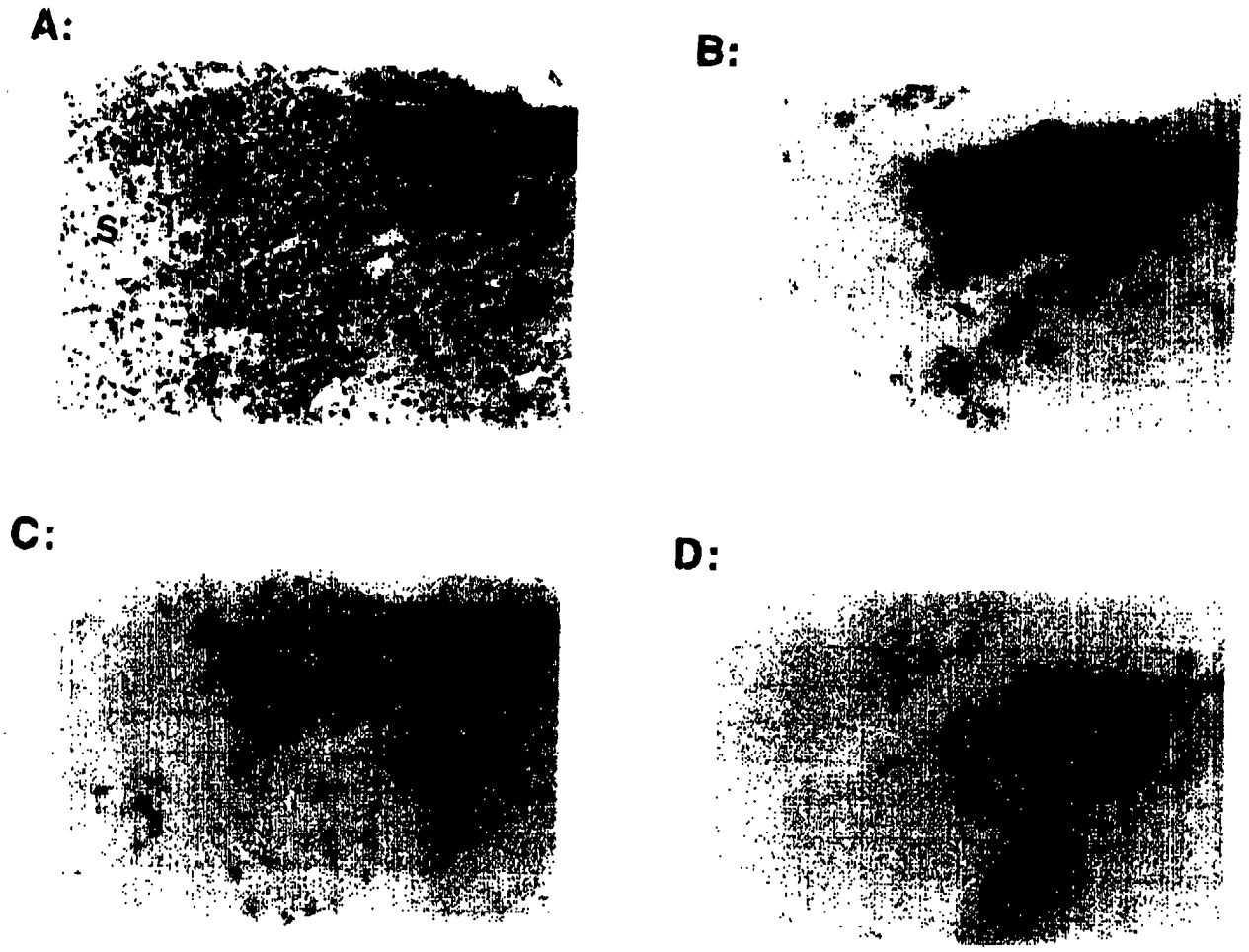

FIGURE 8. Histologic analysis of islet grafts in tolerant hosts. *A*, Tolerance to an islet allograft pretreated with (NL) CTLA4/Fc is not synonymous with the absence of an allograft response (H & E ×200); M, mononuclear cell infiltrate; S, intact islet. *B*, Cells stained with rat anti-mouse CD4 mAb (×200), and *C*, cells stained with rat anti-mouse CD8$^+$ mAb (×200) surround but do not invade the islet allografts in tolerant mCTLA4/Fc-treated hosts. *D*, Immunohistology of graft incubated with the exclusion of a primary Ab (×200).

mCTLA4/Fc and hCTLA4Ig inhibit T cell activation in vitro and can cause donor Ag hyporesponsiveness.

Systemic administration of hCTLA4Ig to mouse recipients of human islet cell xenografts (16) or cardiac allografts (18) has been reported to promote graft tolerance, whereas hCTLA4Ig given to rat recipients of cardiac allografts prolonged engraftment (17). In our studies we have used mCTLA4/Fc to treat islet cell allografts ex vivo before engraftment to test the hypothesis that blockade of CD28/CTLA-4 costimulatory signals, initiated by B7$^+$ donor cells, could prevent rejection without application of systemic immunosuppression. Our aim was to foster direct recognition of graft alloAg in the absence of B7-mediated costimulation, anticipating that this might lead to a long lived anergic state (3, 15) and/or apoptosis (14) of alloAg-specific T cells.

The Fc portion of an Ig, especially the human IgG1 and murine IgG2a isotypes, can facilitate ADCC and CDC in vivo (26). Thus, in theory a mCTLA4/Fcγ2a fusion protein could lyse B7$^+$ donor cells, thereby precluding alloantigen recognition by host T cells in the absence of B7-mediated costimulation. Therefore, in order to test our hypothesis, we used a mutated mCTLA4/Fc that proved to be virtually devoid of the capacity to engage high affinity FcγRI receptors (Fig. 3) or activate C' (Fig. 4). To create a fusion protein that lacks potent ADCC or CDC activity, we introduced mutations in the Fcγ2a domain of mCTLA4/Fc by site-directed mutagenesis. These mutations rendered the resultant (NL) mCTLA4/Fc fusion protein unable to initiate CDC activity and markedly reduced its capacity to bind FcγRI-expressing CHO cells. Both the (L) and (NL) forms of mCTLA4/Fc were equally effective

in blocking T cell proliferation to mitogens in vitro. Thus, the (NL) mCTLA4/Fc should competitively block B7-mediated costimulation without lysing B7$^+$ donor cells.

Interestingly, we found that incubation of fresh islet cell preparations with the (NL) mCTLA4/Fc protein for 1 h before implantation led to a significant incidence of prolonged engraftment ((NL) CTLA4/Fc mean survival time (MST) = 37 days vs media control MST = 21 days or IgG3 MST = 24 days). Indeed, all (NL) mCTLA4/Fc-coated islet allografts (n = 24) demonstrated primary graft function, and 42% of these grafts functioned for more than 150 days (Fig. 7). Furthermore, 50% of those hosts that demonstrated permanent allograft acceptance were tolerant as evidenced by a failure to reject the islet grafts following a donor spleen cell challenge. Moreover, this state of tolerance was donor specific as evidenced by the rejection of third party grafts and the acceptance of a second original donor strain graft. Recipients receiving media-coated (10 of 10) or IgG3-coated (8 of 9) allografts acutely rejected their islet grafts as expected. Eighty-eight percent (7 of 8) of recipients treated with a single 50-μg i.p. dose of (NL) CTLA4/Fc acutely rejected their allografts with a tempo similar to the control groups (Fig. 7). This dose of CTLA4/Fc far exceeds the amount that could have been released from the coated islet graft preparation (see *Materials and Methods*); the graft-protecting effect of the ex vivo treatment could not be simply arise from carry over of (NL) CTLA4/Fc into the circulation of the host.

Why did the pretreatment protocol not achieve a higher degree of permanent engraftment? There are several possibilities. First, B7 proteins may have been up-regulated post-transplantation, leading to an incomplete B7 blockade (22, 30, 31). Second, whereas it has been shown that B7-mediated costimulation represents a crucial pathway of T cell activation, it is possible that other costimulatory ligands can initiate T cell activation and rejection (32). Third, the extent to which recipient T cells are stimulated by alloAg presented in association with MHC proteins on donor APCs (direct pathway) vs host APCs (indirect pathway) is controversial (33). The fact that blockade of B7-mediated costimulation by (NL) mCTLA4/Fc in our model leads to prolonged engraftment, and a significant incidence of permanent engraftment and tolerance, infers an important role for the direct pathway of Ag recognition in the rejection of islet allografts.

A recent attempt to pretreat murine cardiac donors with hCTLA4Ig failed to promote the survival of allogeneic cardiac transplants (18). This failure may be because of differences in the therapeutic ligand (i.e., mouse vs human CTLA4Ig), or the model system (islet vs cardiac grafts). Murine CTLA4/Fc produced by Bristol Myers or (NL) mCTLA4/Fc described in this report binds to B7$^+$ mouse cells with a log fold higher affinity than hCTLA4Ig ((34) and A. Sharpe, unpublished observations). As such the differing results may pertain to the greater efficiency of mCTLA4/Fc vs hCTLA4Ig at blocking B7-mediated costimulation in murine models. With regard to the models, there are two issues to consider. First, owing to the presence of lymph nodes in crude islet cell preparations (22), there is a greater abundance of lymph node-derived DCs in crude islets compared with cardiac allografts. Mature DCs present in lymphoid tissues express far higher levels of B7 proteins than expressed upon immature tissue DCs (30). As such it is possible that pretreatment of donor heart grafts will coat far fewer B7 proteins (on DC in the interstitium) compared with similar treatment of crude islet grafts (13, 30). To further clarify this point, studies are now underway in a murine heart allograft model to test the utility of pretreatment of heart donors with (NL) mCTLA4/Fc.

Second, cardiac, but not islet allografts, are directly vascularized. As a consequence, host APCs have much earlier access to cardiac compared with islet allografts. Hence, indirect presentation of alloAg, through the migration of host APCs into the graft, may be far more important in cardiac as compared with nonvascular islet allografts. As a corollary, islet allograft rejection may be more dependent upon direct alloAg presentation by donor APCs. Thus, strategies directed primarily at disarming effective costimulation mediated by donor APCs may be more successful at abrogating rejection in islet allografts than similar attempts in the cardiac allograft model. In support of the contention that nonislet cell elements (i.e., lymphoid tissue) are primarily responsible for the immunogenicity of islet cell allografts, transplantation of purified islet cell preparations (e.g., handpicked or cultured) leads to permanent engraftment (22, 35).

Pretreatment of islet grafts with (NL) mCTLA4/Fc does not eliminate cellular responses to the allograft. Immunohistologic examination of long-term functioning grafts demonstrates the persistence of cellular responses to the grafted tissue (Fig. 8), a finding that we and others have previously documented (36, 37). The prominent mononuclear cell response tends to encircle but not aggressively infiltrate the islet tissue. Aggressive infiltration, leading to islet cell destruction, is a typical feature of rejection (38). CD4$^+$ cells constitute the major cell population that surrounds the islets, whereas CD8$^+$ cells are only found in a low frequency.

In summary, mCTLA4/Fc proved to be a potent inhibitor of T cell responses to lectin and alloAg in vitro in the mouse system. Our ability to achieve a significant degree of permanent engraftment, using (NL) mCTLA4/Fc to coat B7$^+$ cells before transplantation, supports the notion that B7-mediated costimulation by donor cells is a key triggering event in eliciting allograft rejection. Moreover, long-term engraftment was often achieved in the absence of systemic immunosuppression. This strategy should leave the host immune system intact to respond to other Ags presented upon host B7$^+$ APCs. Finally, it may be of benefit to block B7-mediated costimulation through the use of nonlytic CTLA-4 ligands rather than target B7$^+$

donor cells for lysis, because exposure of recipient T cells to donor alloAg in the absence of costimulation might lead to anergy or apoptosis of host alloAg-specific T cells. This hypothesis is currently being tested in our laboratory. In conclusion, although pretreatment strategies to date have not proved sufficient to induce tolerance in kidney or other primarily vascularized grafts, blocking the function of important costimulatory ligands like B7 ex vivo, before transplantation, might prove to be a useful adjunctive therapy in clinical transplantation. This tactic may limit the magnitude of systemic immunosuppression required to achieve engraftment.

References

1. Hall, B. M. 1991. Cells mediating allograft rejection. *Transplantation 51:1141.*
2. Miller, J. F. A. P. 1961. Immunological function of the thymus. *Lancet 2:748.*
3. Jenkins, M. K., and R. H. Schwartz. 1987. Antigen presentation by chemically modified splenocytes induces antigen-specific T-cell unresponsiveness in vitro and in vivo. *J. Exp. Med. 165:302.*
4. Schwartz, R. H. 1990. A cell culture model for T lymphocyte clonal anergy. *Science 248:1349.*
5. Janeway, C. A. J., and K. Bottomly. 1994. Signals and signs for lymphocyte response. *Cell 76:275.*
6. Freeman, G. J., G. S. Gray, C. D. Gimmi, D. B. Lombard, L. J. Zhou, M. White, J. D. Fingeroth, J. G. Gribben, and L. M. Nadler. 1991. Structure, expression, and T cell costimulatory activity of the murine homologue of the human B lymphocyte activation antigen B7. *J. Exp. Med. 174:625.*
7. Linsley, P. S., W. Brady, L. Grosmaire, A. Aruffo, N. K. Damle, and J. A. Ledbetter. 1991. Binding of the B cell activation antigen B7 to CD28 costimulates T cell proliferation and interleukin 2 mRNA accumulation. *J. Exp. Med. 173:721.*
8. Linsley, P. S., W. Brady, M. Urnes, L. S. Grosmaire, N. K. Damle, and J. A. Ledbetter. 1991. CTLA-4 is a second receptor for the B cell activation antigen B7. *J. Exp. Med. 174:561*
9. Freeman, G. J., F. Borriello, R. J. Hodes, H. Reisner, G. J. O., J. W. Ng, J. Kim, J. M. Goldberg, K. Hathcock, G. Laszlo, L. A. Lombard, S. Wang, G. S. Gray, L. M. Nadler, and A. H. Sharpe. 1993. Murine B7-2, an alternative CTLA4 counter-receptor that costimulates T cell proliferation and interleukin 2 production. *J. Exp. Med. 178:2185.*
10. Boussiotis, V. A., G. J. Freeman, J. G. Gribben, J. Daley, G. Gray, and L. M. Nadler. 1993. Activated human B lymphocytes express three CTLA-4 counterreceptors that costimulate T-cell activation. *Proc. Natl. Acad. Sci. USA 90:11059.*
11. Steinman, R. M. 1991. The dendritic cell system and its role in immunogenicity. *Annu. Rev. Immunol. 9:271.*
12. Macatonia, S. E., C.-Y. Hsieh, K. M. Murphy, and A. O'Garra. 1993. Dendritic cells and macrophages are required for Th1 development of CD4+ T cells from αβ TCR transgenic mice: IL-12 substitution from macrophages to stimulate IFN-γ production is IFN-γ-dependent. *Int. Immunol. 5:1119.*
13. Larsen, C. P., S. C. Ritchie, T. C. Pearson, P. S. Linsley, and R. P. Lowry. 1992. Functional expression of the costimulatory molecule, B7/BB1, on murine dendritic cell populations. *J. Exp. Med. 176:1215.*
14. Liu, Y., and C. A. J. Janeway. 1990. Interferon γ plays a critical role in induced cell death of effector T cell: a possible third mechanism of self-tolerance. *J. Exp. Med. 172:1735.*
15. Tan, P., C. Anasetti, J. A. Hansen, J. Melrose, M. Brunvand, J. Bradshaw, J. A. Ledbetter, and P. S. Linsley. 1993. Induction of alloantigen-specific hyporesponsiveness in human T lymphocytes by blocking interaction of CD28 with its natural ligand B7/BB1. *J. Exp. Med. 177:165.*
16. Lenschow, D. J., Y. Zeng, J. R. Thistlethwaite, A. Montag, W. Brady, M. G. Gibson, P. S. Linsley, and J. A. Bluestone. 1992. Long-term survival of xenogeneic pancreatic islet grafts induced by CTLA4Ig. *Science 257:789.*
17. Turka, L. A., P. S. Linsley, H. Lin, W. Brady, J. M. Leiden, R.-Q. Wei, M. L. Gibson, X.-G. Zheng, S. Myrdal, D. Gordon, T. Bailey, S. F. Bolling, and C. B. Thompson. 1992. T-cell activation by the CD28 ligand B7 is required for cardiac allograft rejection in vivo. *Proc. Natl. Acad. Sci. USA 89:11102.*
18. Pearson, T. C., D. Z. Alexander, K. J. Winn, P. S. Linsley, R. P. Lowry, and C. P. Larsen. 1994. Transplantation tolerance induced by CTLA4-Ig. *Transplantation 57:1701*
19. Brunet, J. F., F. Denizot, M. F. Luciani, M. Roux-Dosseto, M. Suzan, M. G. Mattei, and P. Golstein. 1987. A new member of the immunoglobulin superfamily: CTLA-4. *Nature 328:267.*
20. Duncan, A. R., J. M. Woof, L. J. Partridge, D. R. Burton, and G. Winter. 1988. Localization of the binding site for the human high-affinity Fc receptor on IgG. *Nature 332:563.*
21. Duncan, A. R., and G. Winter. 1988. The binding site for C1q on IgG. *Nature 332:738.*
22. Gotoh, M., T. Maki, S. Satomi, J. Porter, and A. P. Monaco. 1986. Immunological characteristics of purified pancreatic islet grafts. *Transplantation 42:387.*
23. Litchfield, J. T. 1949. A method for rapid graphic solution of time-percent effect curves. *J. Pharmacol. Exp. Ther. 97:399.*
24. Shizuru, J. A., A. K. Gregory, C. T. Chao, and C. G. Fathman. 1987. Islet allograft survival after a single course of treatment of recipient with antibody to L3T4. *Science 237:278.*
25. Bogen, S. A., I. Fogelman, and A. K. Abbas. 1993. Analysis of IL-2-, IL-4- and IFN-γ-producing cells in situ during immune responses to protein antigens. *J. Immunol. 150:4197.*
26. Burton, D. R. 1985. Immunoglobulin G: functional sites. *Mol. Immunol. 22:161.*
27. Mueller, D. L., M. K. Jenkins, and R. H. Schwartz. 1989. Clonal expansion vs functional inactivation. *Annu. Rev. Immunol. 7:445*
28. Paul, W. E. 1993. *Fundamental Immunology*. Raven Press, New York, p. 838.
29. Finck, B. K., P. S. Linsley, and D. Wofsy. 1994. Treatment of murine lupus with CTLA4Ig. *Science 265:1225.*
30. Inaba, K., M. Witmer Pack, M. Inaba, K. S. Hathcock, H. Sakuta, M. Azuma, H. Yagita, K. Okumura, P. S. Linsley, S. Ikehara, S. Muramatsu, R. J. Hodes, and R. M. Steinman. 1994. The tissue distribution of the B7-2 costimulator in mice: abundant expression on dendritic cells in situ and during maturation in vitro. *J. Exp. Med. 180:1849.*
31. Hathcock, K. S., G. Laszlo, C. Pucillo, P. Linsley, and R. J. Hodes. 1994. Comparative analysis of B7-1 and B7-2 costimulatory ligands: expression and function. *J. Exp. Med. 180:631.*
32. Johnson, J. G., and M. K. Jenkins. 1994. Monocytes provide a novel costimulatory signal to T cells that is not mediated by the CD28/B7 interaction. *J. Immunol. 15:429*
33. Shoskes, D. A., and K. J. Wood. 1994. Indirect presentation of MHC antigens in transplantation. *Immunol. Today 15:42*
34. Wallace, P. M., J. S. Johnson, J. F. MacMaster, K. A. Kennedy, P. Gladstone, and P. S. Linsley. 1994. CTLA4Ig treatment ameliorates the lethality of murine graft-versus-host defense across major histocompatibility complex barriers. *Transplantation 58:602.*
35. Lafferty, K. J., S. J. Prowse, and C. J. Simeonovic. 1983. Immunobiology of tissue transplantation: a return to the passenger leukocyte concept. *Annu. Rev. Immunol. 1:143*
36. Pankewycz, O., J. Mackie, R. Hassarjian, J. R. Murphy, T. B. Strom, and V. B. Kelley. 1989. Interleukin-2-diphtheria toxin fusion protein prolongs murine islet cell engraftment. *Transplantation 47:318.*
37. Hao, L., F. Calcinaro, R. G. Gill, E. Eugui, A. C. Allison, and K. J. Lafferty. 1992. Facilitation of specific tolerance induction in adult mice by RS-61443. *Transplantation 54:990*
38. O'Connell, P. J., A. Pacheco-Silva, P. W. Nickerson, R. A. Muggia, M. Bastos, V. Rubin Kelley, and T. B. Strom. 1993. Unmodified pancreatic islet allograft rejection results in the preferential expression of certain T cell activation transcripts. *J. Immunol. 150:1093.*

Proc. Natl. Acad. Sci. USA
Vol. 95, pp. 5929–5934, May 1998
Colloquium Paper

This paper was presented at the colloquium "Computational Biomolecular Science," organized by Russell Doolittle, J. Andrew McCammon, and Peter G. Wolynes, held September 11–13, 1997, sponsored by the National Academy of Sciences at the Arnold and Mabel Beckman Center in Irvine, CA.

Optimizing the stability of single-chain proteins by linker length and composition mutagenesis

CLIFFORD R. ROBINSON* AND ROBERT T. SAUER†

Department of Biology, Massachusetts Institute of Technology, Cambridge MA 02139

ABSTRACT **Linker length and composition were varied in libraries of single-chain Arc repressor, resulting in proteins with effective concentrations ranging over six orders of magnitude (10 μM–10 M). Linkers of 11 residues or more were required for biological activity. Equilibrium stability varied substantially with linker length, reaching a maximum for glycine-rich linkers containing 19 residues. The effects of linker length on equilibrium stability arise from significant and sometimes opposing changes in folding and unfolding kinetics. By fixing the linker length at 19 residues and varying the ratio of Ala/Gly or Ser/Gly in a 16-residue-randomized region, the effects of linker flexibility were examined. In these libraries, composition rather than sequence appears to determine stability. Maximum stability in the Ala/Gly library was observed for a protein containing 11 alanines and five glycines in the randomized region of the linker. In the Ser/Gly library, the most stable protein had seven serines and nine glycines in this region. Analysis of folding and unfolding rates suggests that alanine acts largely by accelerating folding, whereas serine acts predominantly to slow unfolding. These results demonstrate an important role for linker design in determining the stability and folding kinetics of single-chain proteins and suggest strategies for optimizing these parameters.**

The construction of single-chain or hybrid proteins is a potentially powerful method for generating proteins with novel functions and improved properties (1–11). A critical element in such efforts is the design of the peptide linkers that serve to connect different protein domains or subunits. Designed linkers are usually glycine-based peptides with lengths calculated to span the minimum distance between the C terminus of one subunit or domain and the N terminus of the next. How important is linker design in determining the properties of single-chain proteins? Alterations in linker regions have been found to affect the stability, oligomeric state, proteolytic resistance, and solubility of single-chain proteins (12–23), but few systematic investigations of these relationships have been reported. Here, we test the effects of linker design on the stability, protein folding kinetics, and biological activity of single-chain Arc repressor. Wild-type Arc is a dimer with identical subunits, and Arc-L1-Arc is a single-chain variant with a 15-residue linker connecting the subunits (see Fig. 1). The L1 linker of Arc-L1-Arc holds the subunits at an effective concentration (C_{eff}) of 3 mM. By varying linker length and composition, we have isolated single-chain variants with effective subunit concentrations ranging from 10 μM to 10 M, corresponding to changes in the free energy of unfolding (ΔG_u) from 3 to 11 kcal/mol. These differences in stability arise from changes in the folding and unfolding rates, suggesting that linker design can affect protein stability by altering the free energies of both the native and denatured states.

MATERIALS AND METHODS

Cassettes coding for glycine-rich linkers ranging from 3 to 59 residues (Fig. 3*A*) were synthesized using an Applied Biosystems 381A DNA synthesizer and were purified as described (9). A precursor plasmid (pLA3), constructed to facilitate subcloning of linker library cassettes, contains tandem *arc* genes connected by a GGT ACC GGT adapter, which encodes Gly-Thr-Gly and contains unique *Kpn*I and *Age*I restriction sites. Cassette libraries coding for 19-residue linkers with different amounts of Gly or Ala were constructed by synthesizing an oligonucleotide, which formed a hairpin:

```
                                                    AAA
5'-ACACCTTGAGGTACCCGA (GSA)15 GGTACCTAACAGGCG    A
                                3'-CCATGGATTGTCCGC    A
                                                    AAA
```

The underlined sequences are *Kpn*I sites. S represents a mixture of G and C, and thus, the GSA codons encode either glycine (GGA) or alanine (GCA). Three otherwise identical oligonucleotides with different G/C ratios at the randomized positions (1:1; 3:1; 1:3) were synthesized to facilitate identification of a wide range of compositions. A cassette library encoding random combinations of glycine (GGT) and serine (AGT) was constructed in the same manner. Second strand synthesis was carried out using Sequenase v.2.0 (United States Biochemical) for 2 h at 37°C in Sequenase buffer containing 1 mM dNTPs. Cassettes were digested with *Kpn*I and ligated to the *Kpn*I backbone of pLA3. Following transformation into *Escherichia coli* strain HB101, colonies were picked randomly and the appropriate region of the single-chain *arc* gene was sequenced using the dideoxy method. Plasmid DNA encoding in-frame constructs were transformed into *E. coli* strain UA2F for assays of activity *in vivo* (24) and into *E. coli* X90-λO cells for protein expression.

All single-chain Arc proteins contained a $(His)_6$ tail to facilitate purification using Ni-nitrilotriacetic acid chromatography. Protein purification, fluorescence and circular dichroism (CD) spectroscopy, analytical ultracentrifugation, and gel mobility-shift assays were performed as described (9, 25). Protein stability was assayed by urea denaturation by following changes in intrinsic tryptophan fluorescence intensity at 337 nm or CD ellipticity at 234 nm. For these experiments, the protein concentration was 10 μM in buffer containing 50 mM

Abbreviations: C_{eff}, effective concentration; CD, circular dichroism.

*Present address: 3-Dimensional Pharmaceuticals, Exton, PA.
†To whom reprint requests should be addressed. e-mail: bobsauer@mit.edu.

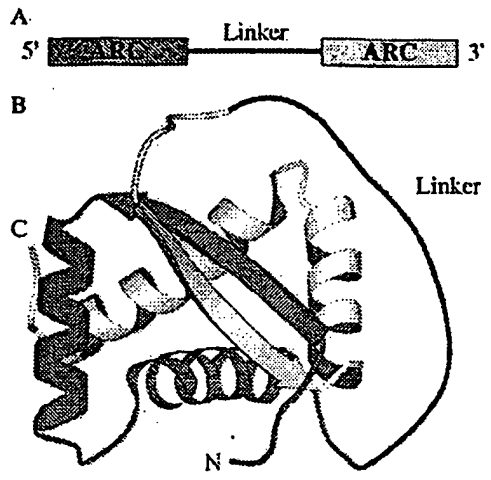

FIG. 1. (*A*) Tandem copies of the *arc* gene connected by DNA encoding a linker region comprise the gene for single-chain Arc repressor. (*B*) One model of how a linker might connect the two subunits (colored gray and white) of single-chain Arc. The positions of the N and C termini are indicated. Prepared using MOLSCRIPT (34) and coordinates of wild-type Arc (33).

Tris·HCl (pH 7.5 at 25°C), 250 mM KCl, and 0.1 mM EDTA (26). Values of ΔG_u and m were obtained by fitting denaturation data to a two-state model by nonlinear least squares methods (26). Effective concentrations were calculated by using the equation $C_{eff} = \exp[(m_2 \bullet \Delta G_1/m_1 - \Delta G_2)/RT]$, where m_1 and ΔG_1 are values for the single-chain protein, and m_2 and ΔG_2 are values for wild-type Arc (1.48 kcal/mol•M and 10.3 kcal/mol, respectively) (26). Stopped-flow kinetic experiments of protein folding and unfolding were monitored by changes in fluorescence at protein concentrations between 1 and 10 μM in the buffer used for stability measurements (26). Unfolding was initiated by urea-jump experiments (mixing ratio 1:10) to yield a final urea concentration of 7 or 9.1 M. Refolding was initiated by mixing protein denatured in 6.0–9.6 M urea with low urea buffer (1:5 ratio) to yield final urea concentrations between 1.0 and 4.5 M. Rate constants were obtained by fitting the kinetic data to single exponentials. In all cases, the residuals of the fits were distributed randomly. For ease of comparison among each library of variants, rates were either measured at a single urea concentration or measured at a series of urea concentrations and extrapolated to this reference concentration by using linear regression of ln(k) vs. [urea] plots ($R > 0.99$).

RESULTS

Variation of Linker Length. A library of single-chain *arc* genes with linkers composed of Gly, Ser, and Thr and lengths varying from 3 to 59 aa was constructed (Fig. 3*A*). The fraction of Gly in different linkers ranges from 66 to 80%. The linkers and corresponding proteins are named LLX and Arc-LLX-Arc (*L*ength *L*ibrary, X = number of residues), respectively. No intracellular expression of the Arc-LL8-Arc protein was detected. Arc-LL3-Arc expressed to high levels but monomers, dimers, and higher-order oligomers were observed following SDS electrophoresis and Western analysis. This behavior may indicate "cross-folding" as has been observed with single-chain antibodies that have very short linkers (27, 28). The remaining 13 proteins in this library were all expressed at high levels and electrophoresed as monomers. The Arc-LLX-Arc variants were tested for repression of transcription of the P_{ant} promoter in *E. coli* strain UA2F, using resistance to streptomycin as an assay of biological activity (24). Arc-LLX-Arc proteins with linkers containing 13 or more residues had wild-type activities. Arc-LL11-Arc was partially active; single-chain molecules with the LL3, LL8, and LL9 linkers were inactive. Modeling studies show that connecting the Arc subunits with linkers shorter than 13 residues would either require the linker to cross the DNA-binding surface of the protein and/or require distortion of the structure.

Single-chain Arcs with linkers LL9–LL59 were purified for biophysical characterization. All of these single-chain proteins had CD and fluorescence spectra similar to wild-type Arc. Arc-LL11-Arc, Arc-LL19-Arc, and Arc-LL31-Arc were analyzed by analytical ultracentrifugation and found to be monomeric at concentrations between 10 and 100 μM (data not shown). Proteins containing the three longest linkers (LL47, LL51, and LL59) tended to precipitate at concentrations >100 μM, possibly because of aggregation caused by cross-folding of the Arc subunits.

The thermodynamic stabilities of Arc-LLX-Arc proteins with linkers from 9 to 57 residues were determined by urea denaturation studies, revealing that the 19-residue linker provides maximal stability. As shown in Fig. 2 for a subset of these proteins, there are large changes in the concentration of urea required for denaturation of proteins with different linker lengths, but the curves are roughly parallel indicating that the denaturant m-values (variation of ΔG_u with urea) are similar. Fig. 3*B* shows the variations of ΔG_u and C_{eff} with linker length. For linkers from 9 to 19 residues, stability of the single-chain protein increased with length. Arc-L9-Arc was the least stable ($\Delta G_u \approx 3$ kcal/mol; $C_{eff} \approx 6$ μM) and Arc-LL19-Arc was the most stable ($\Delta G_u = 8.4$ kcal/mol; $C_{eff} = 80$ mM) of the proteins examined. Increases in linker length past 19 residues resulted in decreasing stability until a plateau was reached at ≈4.5 kcal/mol ($C_{eff} \approx 150$ μM) for linkers between 47 and 59 residues.

The linker-dependent changes in stability arise from changes in both the folding and unfolding rates, as measured in urea-jump, stopped-flow, kinetic experiments. Fig. 3 *C* and *D* show that both the folding and unfolding rate constants vary significantly as the linker length is changed. In 7 M urea, Arc-LL9-Arc unfolds with a rate constant (k_u) of ≈3,000 s^{-1}. As the linker length is increased from 9 to 19, there is a roughly exponential decrease in k_u that spans 3–4 orders of magnitude and reaches a value of ≈1 s^{-1} for Arc-LL19-Arc. Changes in linker length between 19 and 59 residues do not change k_u appreciably. Thus, linkers shorter than 19 residues reduce the

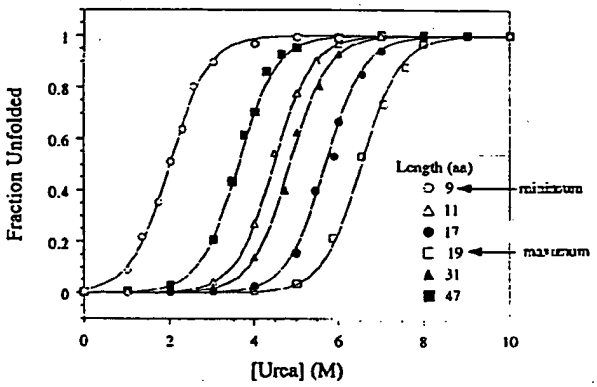

FIG. 2. Linker length has large effects on the stability of single-chain Arc to urea denaturation. The sequences of linkers LL9 (○), LL11 (△), LL17 (●), LL19 (□), LL31 (▲), and LL47 (■) are listed in Fig. 3*A*. Fraction unfolded was calculated by fitting plots of CD ellipticity (234 nm) vs. urea concentration to a two-state-unfolding transition. The solid lines represent the best theoretical fits of the experimental data.

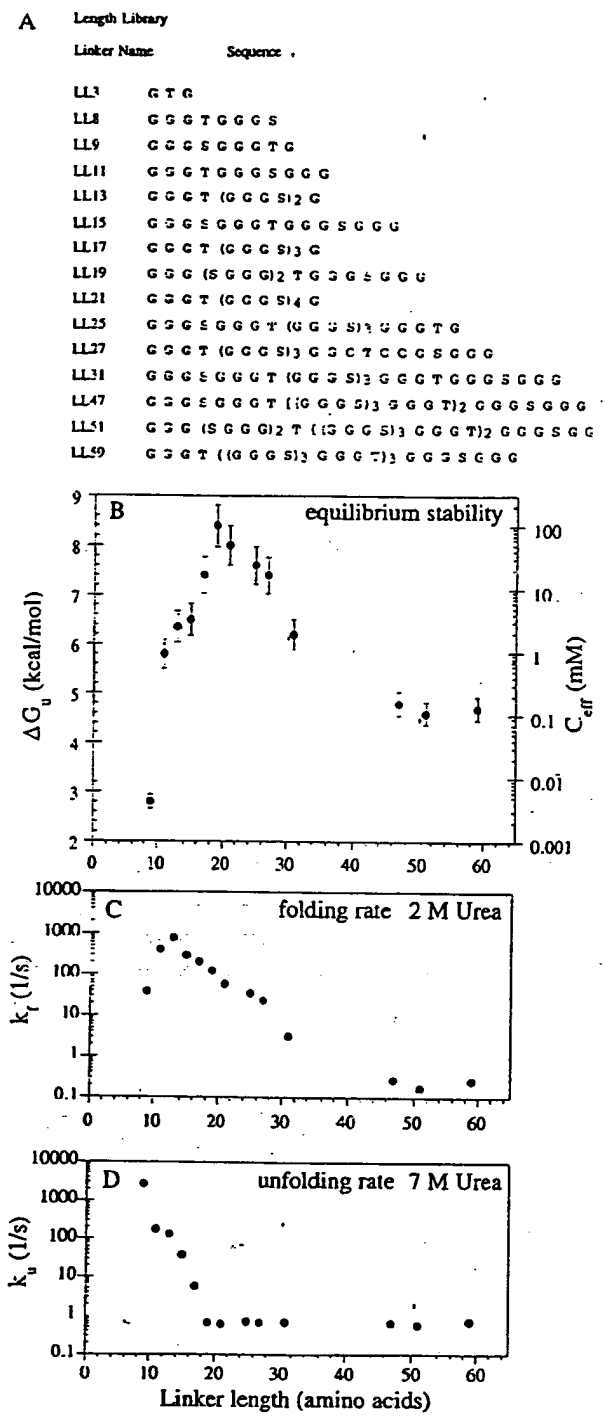

FIG. 3. Properties of linker-length variants of single-chain Arc. (*A*) Linker sequences. (*B*) Equilibrium stability and effective concentration vary with linker length. Error bars indicate one SD from three independent experiments. (*C*) Folding rates in 2 M urea. (*D*) Unfolding rates in 7 M urea. Experimental conditions; protein 1–10 μM, 25°C, 50 mM Tris·HCl (pH 7.5), 250 mM KCl, and 0.1 mM EDTA.

free energy barrier between the native state and the transition state.

The refolding rate (k_f) in 2 M urea has a maximum value of ≈1000 s^{-1} for the Arc-LL13-Arc protein. Decreasing the linker by four residues to a length of nine causes a 30-fold decrease in the folding rate. As the linker length is increased from 13 to 47 residues, the refolding rate also decreases. Over this range, there is a roughly exponential decrease in k_f that spans nearly four orders of magnitude. Little change in k_f is seen for linkers between 47 and 59 residues. These results show that linker length can have large effects on the free energy difference between the denatured state and the transition state. Moreover, the length optima for equilibrium stability (19 residues), refolding (13 residues), and unfolding (19–59 residues) are different. The 19-residue linker provides the greatest equilibrium stability because it is the best compromise between reasonably fast refolding and slow unfolding.

Effects of Linker Composition. To asses the effects of varying the number of glycines in the linker, the length of the linker was fixed at 19 residues and 16 internal positions were randomized between Ala and Gly (ALX library) or between Ser and Gly (SLX library) by using the strategy described in *Materials and Methods*. For these experiments, the libraries were first selected for Arc repressor activity *in vivo* and then the sequences of individual members were determined. Sixteen proteins comprise the ALX library; the linkers in these proteins contain from 3 to 15 alanines (Fig. 4*A*). Ten proteins, with 3-11 serines in the linker region, comprise the SLX library (Fig. 5*A*). All of the Arc-ALX-Arc and Arc-SLX-Arc proteins were expressed at high levels, were purified, and had CD and fluorescence spectra similar to wild-type Arc. In the ALX library, variants with eight or more linker alanines showed some tendency to aggregate during purification and handling but were monomeric at concentrations of 1–20 μM as judged by analytical ultracentrifugation and the concentration independence of equilibrium stability and refolding rates. All other proteins in the ALX and SLX libraries were highly soluble.

The number of non-glycine residues in the 19-residue linker has a significant effect on the equilibrium stability of proteins in both the ALX and SLX libraries, as determined by urea denaturation. In the ALX library (Fig. 4 *A* and *B*), Arc-AL11-Arc, which contains 11 alanines and 5 glycines in the randomized portion of the linker, has the maximum stability ($\Delta G_u \approx$ 11 kcal/mol; $C_{eff} \approx$ 8 M). Arc-AL3-Arc, with 3 alanines and 13 glycines in the randomized region of the linker, is far less stable ($\Delta G_u \approx$ 3 kcal/mol; $C_{eff} \approx$ 10 μM), suggesting that too much linker flexibility is detrimental to stability. Fig. 4*B* shows, however, that stability also decreases when the number of alanines is increased past the optimum value of 11, indicating that linkers that are too inflexible also limit protein stability. The same general trends are observed in the SLX library; proteins with too many or too few glycines are significantly less stable than Arc-SL7-Arc ($\Delta G_u \approx$ 7 kcal/mol; $C_{eff} \approx$ 7 mM). There are, however, two significant differences between the ALX and SLX results. Maximum stability occurs for a protein containing eight glycines in the randomized portion of the linker in the SLX library but for a protein containing only five glycines in this region in the ALX library. Moreover, the stabilities of the most stable variants in each library also differ significantly; Arc-AL11-Arc has an effective concentration that is 1,000-fold greater than Arc-SL7-Arc. We interpret these differences as indicating that the identity of the non-glycine residues in the linker is as important as the number of these residues in determining stability. By contrast, the positions of the glycine and non-glycine residues in the randomized portion of the linker seem to be unimportant. Five pairs of variants in the ALX library and three pairs in the SLX library have the same composition but difference sequences. In each of these cases, the stabilities of these variants (indicated by open and closed symbols in Figs. 4*B* and 5*B*) were found to be within experimental error.

Another significant difference between the ALX and SLX libraries is observed in the unfolding kinetics (Figs. 4*D* and 5*D*). In the ALX library, the unfolding rate of different variants only changes by a factor of 20. In the SLX library, the unfolding rates change by >1,000-fold. In addition, the shapes

A Alanine Library

Linker Name	Sequence
AL3	G T A G G G G G A G G A G G G G G G
AL4	G T A G G G G G G A G G G A G A G G
AL6a	G T A G A G G A G G G G A G G A G A G
AL6b	G T A G G A G A G G G A G A A G G G G
AL7	G T A A G G A G A G G G G A G G A G G
AL8a	G T A G G A A G A G G A G A G A A G G
AL8b	G T A A G A G G A G G G A G G A A A G
AL9a	G T A G A G G G A G G A A A A G A A G
AL9b	G T A G A A G A G A A G A A G G A G G
AL10	G T A A G A G G A A A G A G A A G A G
AL11	G T A A A G A G A A G G A A A G A A G
AL12	G T A A A A G A A A G A A G A A G A G
AL14a	G T A A A A G A G A A A A A A A A A G
AL14b	G T A A A A A A A A G A A A G A A A G
AL15a	G T A A A A A G A A A A A A A A A A G
AL15b	G T A A A A A A A A A A A A A G A A G

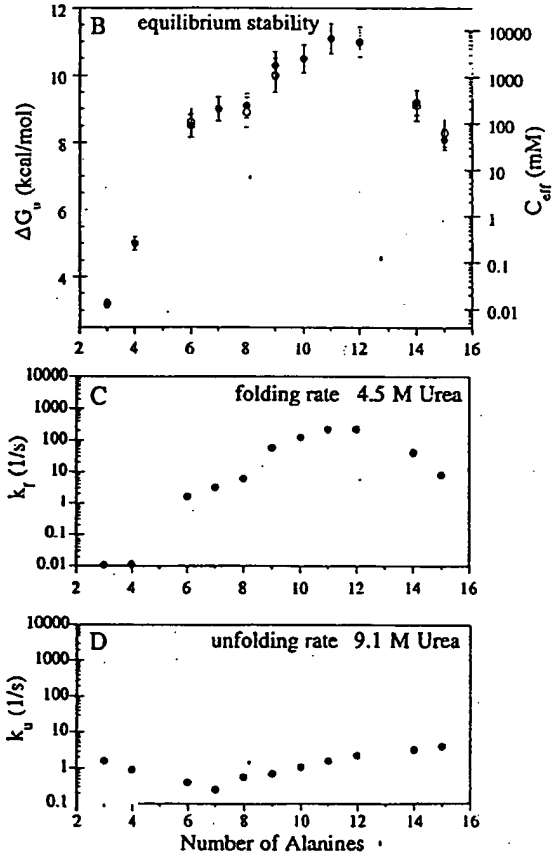

FIG. 4. Properties of ALX variants with 19-residue linkers and differing in Ala/Gly composition numbers of alanines and glycines. (*A*) Linker sequences. (*B*) Equilibrium stability and effective concentration vary with number of alanines. For compositional isomers, closed and open symbols represents "a" and "b" variants, respectively. Error bars indicate one SD from three independent experiments. (*C*) Folding rates in 4.5 M urea. (*D*) Unfolding rates in 9.1 M urea. See Fig. 3 for conditions.

of these plots are very different. The ALX data is concave upward with minimum occurring for the protein with seven

A Serine Library

Linker Name	Sequence
SL3	G T S G G S G G G G G G S G G G
SL4	G T S G G G S G G G S G G S G G G
SL5a	G T S S G G S G G G G S G S G G G
SL5b	G T S G G G G S G G S G S G S G G
SL7	G T S G S S G S G S G G S G S G G
SL8a	G T S S G S G S S G G G S G S G S
SL8b	G T S S G G S G S S S G S G G S G
SL10a	G T S S G S S G S S G G S S S S G
SL10b	G T S S S G S G G S G S S G G S S
SL11	G T S G S G S S S G S S G G S S S

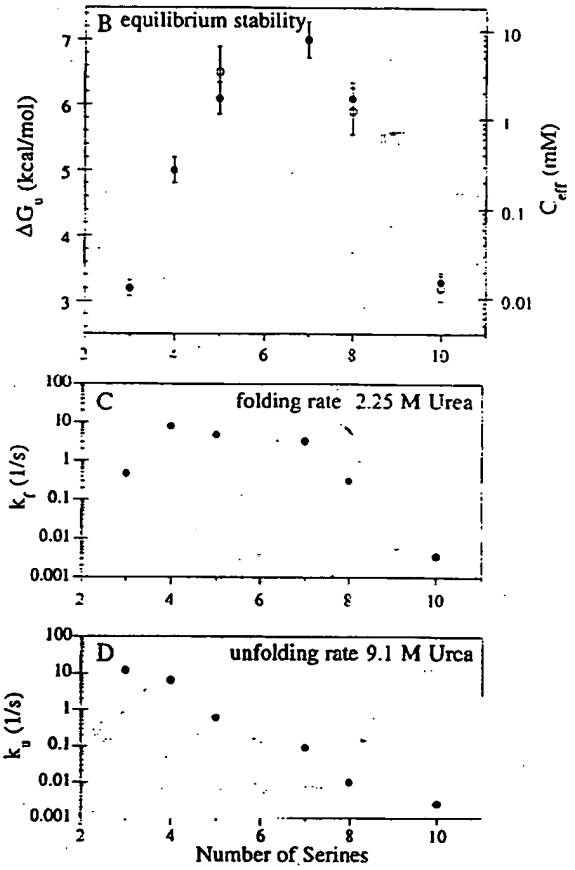

FIG. 5. Properties of SLX variants with 19-residue linkers differing in Ser/Gly composition. (*A*) Linker sequences. (*B*) Equilibrium stability and effective concentration vary with number of serines. For compositional isomers, closed and open symbols represents "a" and "b" variants, respectively. Error bars indicate one SD from three independent experiments. (*C*) Folding rates in 2.25 M urea. (*D*) Unfolding rates in 9.1 M urea. See Fig. 3 for conditions.

alanines and eight glycines in the randomized portion of the linker. In the SLX library, by contrast, k_u decrease exponentially with the number of serines. The rate constants for refolding in the ALX library change by more than five orders of magnitude, reaching a maximum for variants with 11 or 12 alanines in the randomized part of the linker (Fig. 5*C*). Because changes in the unfolding rate are small for the ALX proteins, the changes in equilibrium stability arise almost exclusively from changes in the refolding rate. In the SLX library, variants differ over a 300-fold range in refolding rates with a maximum between four and seven serines. Because

much larger changes are seen in the unfolding rates, the changes in equilibrium stability for the SLX proteins are dominated by the changes in unfolding kinetics. These results emphasize once again that the chemical identity of the non-glycine residues in the linker can have a profound effect on the biophysical properties of the single-chain proteins.

DISCUSSION

Linker length and composition exert a surprisingly large influence on the stability of single-chain Arc repressor. In the LLX linker length library, the most stable protein has a linker of 19 residues, and adding or deleting a few amino acids decreases stability (Fig. 3*B*). These length effects on stability arise from changes in the folding and unfolding rates. In the regime from 59 to 13 residues, shortening the linker accelerates folding. This observation is explained most simply if the denatured subunit domains are constrained to smaller and smaller regions of conformation space by shorter linkers and thus require less random sampling before essential collisions required for folding occur. We note, however, that the length dependence of the stability of single-chain Arc variants in this regime is significantly steeper than for loop-length variants of single-chain Rop (29) and is modeled poorly by simple, random walk, entropic considerations (30). As the linker length decreases from 13 to 11 to 9 residues, there is a decrease in the folding rate of the corresponding Arc-LLX-Arc protein. At some point, the linkers must become too short to connect the subunits in the native conformation without strain. In fact, in the linker length regime from 19 to 9 residues, the unfolding rates of the corresponding Arc-LLX-Arc proteins increases exponentially as the linkers become shorter, suggesting that shorter tethers in this length range introduce more and more strain into the native structure. Presumably, proteins with the LL17, LL15, and LL13 linkers do not show decreased folding rates because of compensating changes in conformational search efficiency.

Glycine is generally used in designed linkers because the absence of a β-carbon permits the polypeptide backbone to access dihedral angles that are energetically forbidden for other amino acids (31). Thus, a glycine-rich linker will be more flexible than a linker of comparable length composed of non-glycine residues. Our results, however, indicate that too much linker flexibility is detrimental to single-chain protein stability. In the ALX (alanine/glycine) library, maximum stability was observed when the 16-residue-randomized region contained 11 alanines and 5 glycines. In the SLX (serine/glycine) library, the most stable protein had seven serines and nine glycines in the randomized portion of the linker. In both libraries, plots of stability vs. the number of non-glycine residues are relatively regular and proteins with the same linker compositions have comparable stabilities (Figs. 4*B* and 5*B*). Both observations suggest that it is the composition rather than the sequence of the linker that is important in determining stability. A single exception to this generalization is provided by Arc-LL19-Arc and Arc-SL3-Arc, which have the same composition but stabilities differing by 3.4 kcal/mol. The first three residues of the linker are Gly-Thr-Ser in Arc-SL3-Arc, which has lower stability, and Gly-Gly-Gly in Arc-LL19-Arc, suggesting that the conformational flexibility imparted by glycine may be important at the junction between C terminus of the first subunit and the N terminus of the linker.

In the ALX library, the main effects of alanine composition on stability result from changes in the refolding rate. For example, as the number of alanines in the linker increases from 3 to 11, the folding rates of the corresponding proteins increase by 30,000-fold. Alanine restricts the number of allowed conformations of the linker compared with glycine and, in this length regime, probably accelerates the conformational search that occurs during folding. Increasing the number of alanines to 14 or 15 then reduces the folding rate, probably because these linkers become too inflexible. When serine is substituted for glycine, there are also effects on the refolding rate but with several differences: the optimal number of serines is smaller than the optimal number of alanines (7 Ser vs. 11 Ala), the difference between the fastest and slowest folders are smaller (≈2,000-fold for SLX vs, ≈30,000-fold for ALX), and the maximum folding rates are different (in 2.25 M urea, the fastest ALX protein folds ≈250 times faster than the fastest SLX protein). Clearly, alanine and serine affect linker flexibility in rather different ways.

Large differences between alanine and serine are also apparent when comparing effects on the unfolding rate. As the number of serines in the linker increases, the unfolding rate continues to decrease over a 5,000-fold range (Fig. 5*D*). By contrast, in the alanine library, the minimum unfolding rate is observed for a protein with seven alanines and the total change between the slowest and fastest unfolders is only 15-fold. We presume that the ability of serine to form hydrogen bonds allows formation of new stabilizing interactions in the native state but whether these interactions are within the linker or involve interactions between the linker and the body of the single-chain protein is unknown. Because alanines in the linker primarily affect folding rates whereas serine has the largest effects on unfolding rates, it seems possible that optimizing the composition of Gly, Ser, and Ala in a linker library might produce single-chain molecules with even greater stabilities than those described here. Preliminary studies also suggest that the effects of length and composition may be interdependent. For example, linkers of different lengths may have different optimal compositions.

Variations in linker length or composition caused no significant changes in repressor activity *in vivo* except in proteins with linkers shorter than 11 residues. In gel mobility-shift assays, Arc-LL19-Arc and Arc-LA11-Arc, which have 19-residue linkers, bound operator DNA as strongly as wild-type Arc dimers (data not shown). In earlier work, however, we found that Arc-L1-Arc (which is identical to Arc-LL15-Arc) had a 10-fold enhanced affinity for operator DNA (9, 26). In single-chain Arc, the linker connects the N-terminal arm of the second subunit to the C terminus of the first subunit; in wild-type Arc, this N-terminal arm is disordered in solution (32) but folds against the operator in the protein-DNA complex (33). The L1/LL15 linker may increase operator affinity by helping to restrict the conformation of the arm in solution, thereby reducing the entropic penalty for ordering the arm upon DNA binding (9). By this model, lengthening the linker to 19 residues probably reduces constraints on the arm conformation.

In summary, we find that changes in linker length and composition can produce substantial changes in the stability and folding kinetics of single-chain Arc. Poly-glycine linkers maximize the conformational freedom of the polypeptide backbone but do not result in optimal stability. For single-chain or hybrid protein designs that have folding problems, alterations in linker length and/or composition should provide a useful method for increasing stability.

We thank David Goldenberg for helpful discussions. This work was supported by an National Institutes of Health postdoctoral fellowship (to C.R.R.) and by National Institutes of Health Grant AI-15706 (to R.T.S.).

1. Bird, R. E., Hardman, K. D., Jacobson, J. W., Johnson, S., Kaufman, B. M., Lee, S.-M., Lee, T., Pope, S. H., Riordan, G. S. & Whitlow, M. (1988) *Science* 242, 423–426.
2. Pomerantz, J. L., Sharp, P. A. & Pabo, C. O. (1995) *Science* 267, 93–96.
3. Predki, P. F. & Regan, L. (1995) *Biochem.* 34, 9834–9839.

4. Hallewell, R. A., Laria, I., Tabrizi, A., Carlin, C., Getzoff, E. D., Tainer, J. A., Cousens, L. S. & Mullenbach, G. T. (1989) *J. Biol. Chem.* **264**, 5260–5268.
5. Bizub, D., Weber, I. T., Cameron, C. E., Leis, J. P. & Skalka, A. M. (1991) *J. Biol. Chem.* **266**, 4951–4958.
6. Kim, S.-H., Kang, C.-H., Kim, R., Cho, J. M., Lee, Y.-B. & Lee, T.-K. (1989) *Protein Eng.* **2**, 571–575.
7. Liang, H., Sandberg, W. S. & Terwillinger, T. C. (1993) *Proc. Natl. Acad. Sci. USA* **90**, 7010–7014.
8. Toth, M. J. & Schimmel, P. (1986) *J. Biol. Chem.* **261**, 6643–6646.
9. Robinson, C. R. & Sauer, R. T. (1996) *Biochem.* **35**, 109–116.
10. O'Shea, E. K., Rutkowski, R. & Kim, P. S. (1992) *Cell* **68**, 699–708.
11. Pantoliano, M. W., Bird, R. E., Johnson, S., Asel, E. D., Dodd, S. W., Wood, J. F. & Hardman, K. D. (1991) *Biochem.* **30**, 10117–10125.
12. Mallender, W. D. & Voss, E. W., Jr. (1994) *J. Biol. Chem.* **269**, 199–206.
13. Rumbley, C. A., Denzin, L. K., Yantz, L., Tetin, S. Y. & Voss, E. W., Jr. (1993) *J. Biol. Chem.* **268**, 13667–13674.
14. Stemmer, W. P., Morris, S. K. & Wilson, B. S. (1993) *BioTechniques* **14**, 256–265.
15. Lieschke, G. J., Rao, P. K., Gately, M. K. & Mulligan, R. C. (1997) *Nat. Biotech.* **15**, 35–40.
16. Eustance, R. J. & Schleif, R. F. (1996) *J. Bacteriol.* **178**, 7025–7030.
17. Govindaraj, S. & Poulos, T. L. (1996) *Protein Sci.* **5**, 1389–1393.
18. Kortt, A. A., Lah, M., Oddie, G. W., Gruen, C. L., Burns, J. E., Pearce, L. A., Atwell, J. L., McCoy, A. J., Howlett, G. J., Metzger, D. W., *et al.* (1997) *Protein Eng.* **10**, 423–433.
19. Whitlow, M., Bell, B. A., Feng, S.-L., Filpula, D., Hardman, K. D., Hubert, S. L., Rollence, M. L., Wood, J. F., Schott, M. E., Milenic, D. E., *et al.* (1993) *Protein Eng.* **6**, 989–995.
20. Deonarain, M. P., Rowlinson-Busza, G., George, A. J. T. & Epenetos, A. A. (1997) *Protein Eng.* **10**, 89–98.
21. Tang, Y., Jiang, N., Parakh, C. & Hilvert, D. (1996) *J. Biol. Chem.* **271**, 15682–15686.
22. Newton, D. L., Xue, Y., Olson, K. A., Fett, J. W. & Rybak, S. M. (1996) *Biochem.* **35**, 545–553.
23. Huston, J. S., McCartney, J., Tai, M.-S., Mottola-Hartshorn, C., Jin, D., Warren, F., Keck, P. & Oppermann, H. (1993) *Int. Rev. Immunol.* **10**, 195–217.
24. Bowie, J. U. & Sauer, R. T. (1989) *Proc. Natl. Acad. Sci. USA* **86**, 2152–2156.
25. Milla, M. E., Brown, B. M. & Sauer, R. T. (1993) *Protein Sci.* **2**, 2198–2205.
26. Robinson, C. R. & Sauer, R. T. (1996) *Biochem.* **35**, 13878–13884.
27. Poljak, R. J. (1994) *Structure* **2**, 1121–1123.
28. Perisic, O., Webb, P. A., Holliger, P., Winter, G. & Williams, R. L. (1994) *Structure* **2**, 1217–1226.
29. Nagi, A. D. & Regan, L. (1997) *Fold. Des.* **2**, 67–75.
30. Chan, H. S. & Dill, K. A. (1988) *J. Chem. Phys.* **90**, 492–509.
31. Ramachandran, G. N. & Sasisekharan, V. (1968) *Adv. Protein Chem.* **23**, 283–437.
32. Breg, J. N., van Opheusden, J. H. J., Burgering, M. J. M., Roelens, R. & Kaptein, R. (1990) *Nature (London)* **346**, 586–589.
33. Raumann, B. E., Rould, M. A., Pabo, C. O. & Sauer, R. T. (1994) *Nature (London)* **367**, 754–757.
34. Kraulis, P. J. (1991) *J. Appl. Cryst.* **24**, 946–950.

THE JOURNAL OF BIOLOGICAL CHEMISTRY Vol. 273, No. 18, Issue of May 1, pp. 11173–11176, 1998
© 1998 by The American Society for Biochemistry and Molecular Biology, Inc. Printed in U.S.A.

Homodimerization Restores Biological Activity to an Inactive Erythropoietin Mutant*

(Received for publication, October 31, 1997, and in revised form, January 15, 1998)

Huawei Qiu‡, Adam Belanger, Hae-Won P. Yoon, and H. Franklin Bunn§

From the Hematology Division, Brigham and Women's Hospital, Harvard Medical School, Boston, Massachusetts 02115

Erythropoietin (Epo) is believed to transduce a signal by bringing two Epo receptors into close proximity, enabling cross-phosphorylation. We compared monomeric Epos with homodimers in which two Epo monomers are linked by polyglycine. Monomeric Epo mutant R103A is unable to support Epo-dependent cell growth or trigger Janus kinase 2 and STAT5 activation, even at concentrations greater than 7,000 times that sufficient for wild-type Epo activity. In contrast, R103A homodimer induces proliferation and transduces signal at concentrations similar to that of wild-type Epo monomer and homodimer. These experiments show that two discrete domains on Epo are required for receptor binding and activation. Our results also suggest that the EpoR can be dimerized by different forms and sizes of molecules, as long as *two* recognition motifs are provided in the same molecule. Design of other dimeric molecules may enhance our understanding of cytokine specificity and signal transduction.

The biological activity of a number of cytokines depends upon ligand-induced aggregation of their cognate receptors, as exemplified most convincingly by structural and biochemical studies of human growth hormone and its receptor (1–5). A similar mechanism has been proposed for receptor activation by erythropoietin (Epo),[1] the primary regulator of red blood cell production (6–9). The binding of Epo to its receptor (EpoR) initiates a complex signal transduction cascade that includes the JAK-STAT, phosphatidylinositol-3 kinase, and Ras pathways (10, 11). Epo-specific signal transduction can be induced in the absence of ligand by a mutant EpoR in which a cysteine replacement in the extracellular domain enables two receptor molecules to form a disulfide bond (12). Moreover, a synthetic peptide bearing no resemblance to Epo can also transduce a signal by binding to two EpoR molecules (13, 14).

These observations raise the question of how a nonsymmetric protein monomer specifically activates its cognate receptor on the cell surface. There is no direct information to date on Epo's three-dimensional structure. Expression and characterization of a large number of site-directed Epo mutants support a four α-helical bundle structural model (15), resembling that of other cytokines (16). Several of these Epo mutants have been shown to be deficient or lacking in biological activity (17–20). These structure-function studies have led to the proposal of two domains on Epo that bind to its receptor: one at Arg^{150}, Gly^{151}, Lys^{152}, and the other at Arg^{14}, Arg^{103}, and possibly Ser^{104} (18–20). Mutants that nullify either of the two domains would be unable to bind to two EpoR molecules. Among the mutants tested to date, R103A has the lowest specific bioactivity (17–19). No proliferation activity was detectable even at high concentrations. Despite this, R103A Epo is able to bind tightly to its receptor (19) and therefore is likely to retain one high affinity domain. We designed dimeric forms of Epo in which two R103A Epo mutants were tandemly attached by a flexible isopeptide linkage and asked whether the presence of a second postulated high affinity binding motif in the same molecule could resurrect R103A's activity. We demonstrate that the Arg^{103} homodimers were biologically active, stimulating proliferation of human leukemia cell line UT7/Epo, and transducing Epo-specific signaling. These results provide direct evidence for the two-domain model of erythropoietin function.

EXPERIMENTAL PROCEDURES

Plasmids—The construction of plasmid vectors expressing monomeric Epos was reported previously (15, 18). Briefly, a 943-base pair *EcoRI-BglII* fragment, which includes the complete coding sequence of the wild-type human erythropoietin as well as untranslated regions 216 base pairs upstream and 183 base pairs downstream, was inserted into the mammalian expression plasmid pSG5 (Stratagene) and designated pSG5-EPO/WT. To enhance Epo purification, a His_6 tag was engineered immediately adjacent to the C terminus by means of PCR with oligonucleotide primers *Eco*RT (5′-GGC GAA TTC CCC GGA GCC G-3′) and *Bam*HisB (5′-TCA CGC GGA TCC TCA GTG GTG GTG GTG GTG GTG TCT GTC CCC TGT CCT GCA GGC-3′). The amplification products were purified and inserted into the *Eco*RI and *Bam*HI site of pSG5, and the resulting vector was designated pSG5-EPO.His/WT. pSG5-EPO.His/R103A was made by the same pair of PCR primers using pSG5-EPO/R103A as template.

Plasmids containing dimeric Epo DNA were made from a three-way ligation of two PCR-amplified monomeric units into *Eco*RI and *Bam*HI sites of parental plasmid pSG5. pSG5-Epo/WT and pSG5-Epo/R103A DNA were used as templates. The primers used were: *Eco*RT (see above) and *Bst*EB (5′-GAA GTG CGG TCG CCT GTC CTG CAG GCC TC-3′) for the first monomer and *Bst*ET/Gly_n (*e.g.* *Bst*E/Gly_3: 5′-GAA GTG CGA CCG AGC CGG GGG CGC CCC ACC ACG CC-3′; the primer sequences for 5, 7, and 9 Gly were similar to the Gly_3 primer and thus not shown) and *Bam*HB (5′-TCA CGC GGA TCC CTA TCA TCT GTC CCC TGT CCT GCA GGC-3′) for the second monomer. The two PCR products were digested with *Eco*RI/*Bst*EI and *Bst*EI/*Bam*HI, respectively, and ligated together with *Eco*RI/*Bam*HI digested pSG5 vector. The His_6-tagged Epo DNA was prepared by PCR in the same way except that *Bam*HB was replaced with *Bam*HisB primer (see above). In the preparation of the R103A dimers, *Bam*(-Arg)HisB(5′-TCA CGC GGA TCC TCA GTG GTG GTG GTG GTG GTG GTC CCC TGT CCT GCA GGC CTC-3′) was used to make a polyhistidine tag adjacent to Asp^{165} of the second monomer. This was done to avoid the suspected cleavage of the poly-His tag at Arg^{166} which is normally the last amino acid of

* This work was supported by National Institutes of Health Grant RO1 HL 42949-09 (to H. F. B.). The costs of publication of this article were defrayed in part by the payment of page charges. This article must therefore be hereby marked "*advertisement*" in accordance with 18 U.S.C. Section 1734 solely to indicate this fact.

‡ Recipient of National Institutes of Health NRSA Award HL09674-02.

§ To whom correspondence should be addressed: Hematology Division, Brigham and Women's Hospital, LMRC-223, 221 Longwood Ave., Boston, MA 02115. Tel.: 617-732-5841; Fax: 617-739-0748; E-mail: bunn@calvin.bwh.harvard.edu.

[1] The abbreviations used are: Epo, erythropoietin; EpoR, erythropoietin receptor; JAK2, Janus kinase 2; STAT, signal transducer and activator of transcription; PCR, polymerase chain reaction; RIA, radioimmunoassay.

Epo immediately N-terminal to the engineered His tag.[3] The Ala mutation in both monomeric units of R103A dimer was confirmed by didoxy sequencing of *BsiE*-digested and purified monomeric DNA fragments.

Production of Monomeric and Dimeric Epo in Mammalian Cells—COS7 cells were maintained in Dulbecco's modified Eagle's medium (Life Technologies, Inc.) containing 15% fetal bovine serum and 1% penicillin/streptomycin. For transient expression of Epo, COS7 cells were grown to 60–80% confluency, transfected with 20 μg of recombinant plasmid DNA per 10-cm dish using the calcium phosphate precipitation protocol. 20 μg plasmid pADVantage (Promega) were co-transfected to enhance the yield of protein production. 72 h after transfection, the medium was filtered and subjected to radioimmunoassay (RIA) to determine secreted Epo concentration. For the transfection of plasmids containing His_6-tagged Epo, spent medium was removed 24 h after transfection, and COS7 cells were allowed to grow for 2 more days in serum-free medium before collecting the supernatant. Medium containing His_6-tagged proteins was loaded onto a Ni-nitrilotriacetic acid metal Chelex column (Qiagen) for affinity purification.

Bioassays—The dose-dependent proliferation activities of wt Epo and Epo mutants were assayed *in vitro* using an Epo-responsive target cell UT7/Epo, a human cell line derived from the bone marrow of a patient with acute megakaryoblastic leukemia (22). Briefly, cells were washed with PBS and mixed with various amounts of Epo in a 96-well plate, with approximately 10^4 cells/well; after 72 h of incubation, cellular growth was determined by [^{3}H]thymidine (NEN Life Science Products) incorporation (23) and colorimetric proliferation assay (Promega).

Immunoprecipitation and Western Blot—1×10^7 UT7/EPO cells were starved in medium lacking Epo for 16 h and then treated with various forms of Epo for 5 min. Cells were lysed in 0.8 ml of lysis buffer containing 1% Triton X-100 and 100 μM sodium vanadate, and immunoprecipitated with antibody against JAK2 (Upstate Biotechnology). Samples were electrophoresed on a 7% SDS-polyacrylamide gel and Western blotted with an antibody against phosphotyrosine (4G10, Upstate Biotechnology) using enhanced chemical luminescence (Promega).

Electrophoretic Mobility Shift Assay—UT7/Epo cells were starved overnight and stimulated with Epo for 5 min. Cells were washed, collected, and used for preparation of nuclear extracts. Nuclear extracts (5 μg) were incubated with 0.25 ng of ^{32}P-labeled STAT5 consensus binding sequence (5'-AGA TTT CTA GGA ATT CAA TCC-3', Santa Cruz Biotechnology) for 20 min at room temperature and electrophoresed on a 5% polyacrylamide gel in 0.5× TBE buffer. In the supershift experiment, 1 μg of anti-STAT5 (Santa Cruz Biotechnology) antibody was added following the initial incubation and reincubated at room temperature for another 15 min before electrophoresis.

RESULTS

Expression of Dimeric Epo in COS7 Cells—The R103A dimers and WT dimers were constructed by PCR (Fig. 1) and prepared by transient expression and secretion in mammalian COS7 cells. Concentration of Epo products was determined by a RIA using a polyclonal antiserum against Epo (15, 21). Studies employing conformation-dependent monoclonal antibodies indicate that R103A is properly folded into native tertiary structure (24, 25) and therefore would be expected to bind as avidly as WT Epo to the polyclonal antiserum. We found that dimeric Epos were secreted from COS7 cells at levels comparable to that of monomeric Epo (in the range of 150–500 units/ml). The fact that these dimers are recognized by Epo antiserum in the RIA suggests that their tertiary structures are intact.

Epo-dependent Cell Proliferation—The biological activity of R103A dimer was assessed in two ways: 1) *in vitro* proliferation in UT7/Epo cells, an Epo-responsive human cell line (22); and 2) activation of Epo-specific signal transduction monitored by Jak2 phosphorylation and activation of STAT5 binding to DNA.

The proliferation bioassay shown in Fig. 2 compares the dose response curves of UT7/Epo cells exposed to WT Epo and the R103A mutant, both as monomers and as homodimers. Proliferation generally requires >50 milliunits/ml monomeric WT Epo (EC_{50} = 105 milliunits/ml). A similar biological effect was observed at the same concentrations of dimeric WT Epo (EC_{50} = 185 milliunits/ml). As shown previously (17–19), monomeric R103A was completely inert even at a concentration of 350,000 milliunits/ml, at least 7,000 times that sufficient for WT Epo activity (Fig. 2). In contrast, dimeric R103A was biologically active at ~150 milliunits/ml (EC_{50} ~= 400 milliunits/ml), slightly higher than that required for dimeric WT Epo. The biological activities of the dimeric WT Epo and dimeric R103A were not affected by the number (3–7) of glycine spacers.

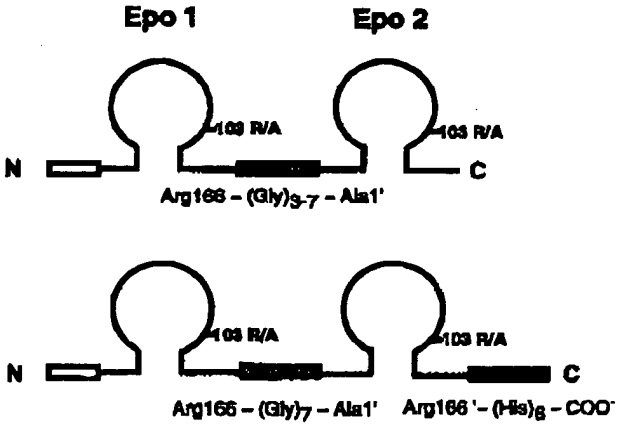

FIG. 1. **Depiction of dimeric Epo molecules used in this study.** Two copies of the full coding sequence for WT (*103 R*) or mutant (*103 A*) Epo are separated by a sequence encoding 3 to 7 glycine residues (*striped rectangle*). The Epo signal peptide sequence (*open rectangle*) at the 5' end enabled efficient cellular processing and export. The Gly_7-linked dimers were also prepared with a polyhistidine sequence His_6 at the 3' end (*shaded rectangle*) that enabled purification and immunologic detection.

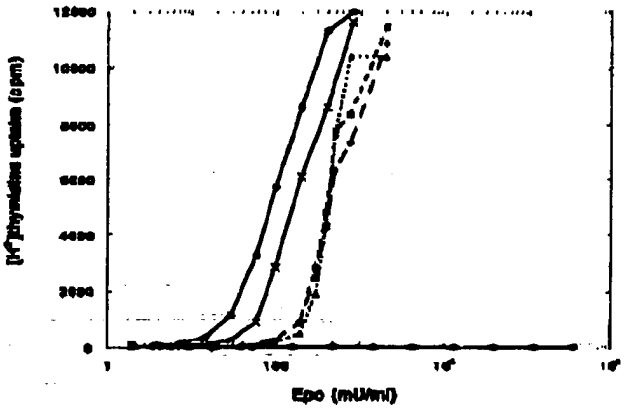

FIG. 2. **Comparison of proliferative biological activities of WT and mutant (R103A) monomeric and dimeric Epo molecules.** Epo-dependent proliferation was assayed in UT7/Epo cells. Incorporation of [^{3}H]thymidine was monitored after 72 h of incubation with increasing concentrations of Epo. ●, WT Epo monomer; ×, WT Epo dimer Gly_7; ■, R103A dimer Gly_3; ◆, R103A dimer Gly_5; ▲, R103A dimer Gly_7; ○, R103A monomer.

JAK2 Phosphorylation and STAT5 Activation upon Epo Stimulation—Analysis of Epo-dependent signal transduction, as shown in Fig. 3, *A* and *B*, was in full agreement with the cell proliferation results described above. Phosphorylation of JAK2, a member of the Janus kinase family, is thought to be the first step of Epo-specific signal transduction upon EpoR activation. As expected from previous studies (26), the addition of WT Epo to UT7/Epo cells, in doses as low as 0.5 unit/ml, resulted in

[3] The biological activity of Epo is unaffected either by mutations at the C terminus including deletion of the C-terminal Arg or by the addition of poly-His to the C terminus (15).

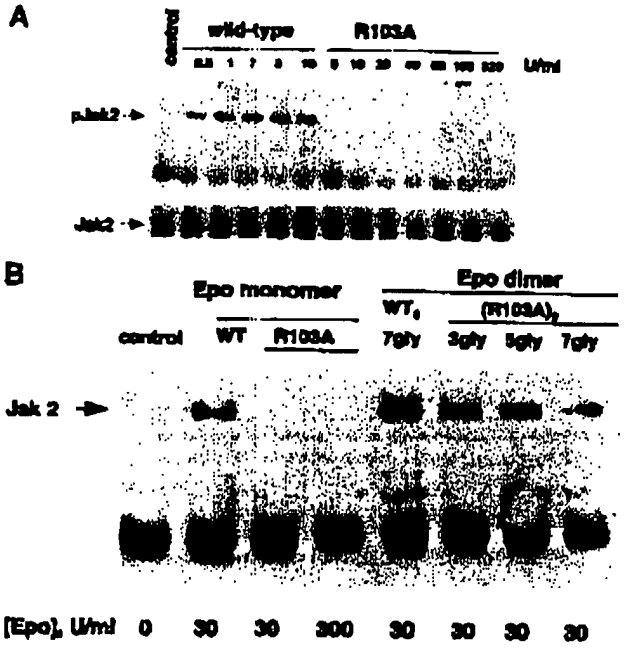

FIG. 3. **Tyrosine phosphorylation of Janus kinase 2 (JAK2) protein upon Epo monomer (*panel A*) and dimer (*panel B*) stimulation.** *A*, UT7/Epo cells were starved overnight and collected 5 min after addition of WT or mutant (R103A) monomeric Epo. The cell lysate were subjected to immunoprecipitation with JAK2 antibody and Western blotted with antibody against phosphotyrosine (*top*) and JAK2 (*bottom*). *B*, comparison of JAK2 phosphorylation stimulated by WT and R103A Epo monomers and dimers.

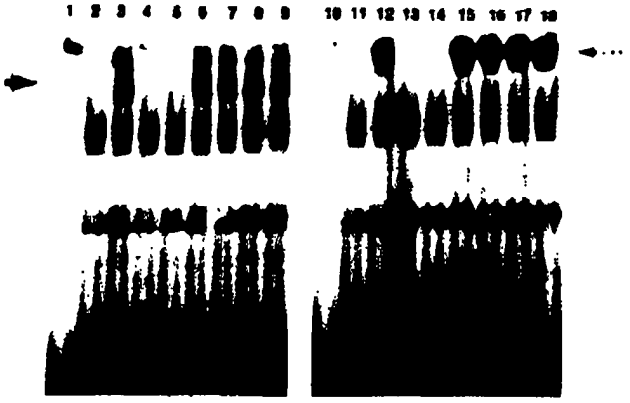

FIG. 4. **Electrophoretic mobility shift assay of nuclear extracts made from UT7/Epo cells treated with WT or R103A monomeric and dimeric Epos.** 30 units/ml Epo was used unless otherwise specified. ^{32}P-Labeled STAT5 consensus sequence was used as the probe. Migration of STAT5 protein-DNA complex is marked by a *solid arrow*. *Lane 1*, buffer control; *lane 2*, UT7/Epo nuclear extract with no Epo treatment; *lane 3*, WT monomer; *lanes 4* and *5*, R103A monomer, 30 and 300 units/ml, respectively; *lane 6*, WT dimer; *lanes 7–9*, R103A dimer with 3, 5, and 7 Gly linkers. *Lanes 10–18* are the same as *lanes 1–9* except that an antibody against STAT5 proteins was added to supershift the protein-DNA complex (marked by *dashed arrow*).

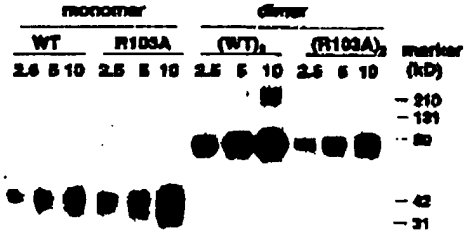

FIG. 5. **Comparison of monomer and dimer Epo concentration using Western blot.** Epo monomer and dimer samples estimated by RIA to contain the same amounts of Epo (2.5, 5, and 10 units of each species) were run on a denaturing SDS-PAGE gel and blotted with monoclonal antibodies against the poly-His tag.

prompt tyrosine phosphorylation of JAK2. In contrast, addition of up to a 640-fold higher dose of monomeric R103A failed to induce JAK2 phosphorylation (Fig. 3*A*). However, in keeping with the bioassay results in Fig. 2*A*, dimers of both WT Epo and R103A, when added to UT7/Epo cells, elicited robust phosphorylation of JAK2 (Fig. 3*B*).

Several signal transduction pathways subsequent to JAK2 phosphorylation have been shown to be activated by Epo (10, 11). One which has been thoroughly studied is the JAK-STAT pathway in which STAT5 protein is recruited by activated EpoR and becomes phosphorylated by JAK2. Phosphorylated and dimerized STAT5 protein is translocated into the nucleus where it binds to consensus DNA sequences and transactivates gene expression. To test whether the Epo dimers utilize the same pathway, the binding of activated STAT5 protein to its consensus promoter sequence was analyzed by electrophoretic mobility shift assay, as shown in Fig. 4. R103A dimers induced STAT5 activation, suggesting that, like wild-type Epo, they triggered signaling along the JAK-STAT pathway.

Immunoblot of the Engineered Tag for Confirmation of Protein Concentration—To rule out a significant error in our measurement of Epo concentration by immunoassay, we devised an independent way of measuring the absolute concentration of our recombinant Epo products. The coding regions were extended to include six histidine residues at the C terminus of monomeric and dimeric Epo (attached to Asp^{165} or Arg^{165} of the second monomer unit) (Fig. 1). The C-terminal poly-His tag does not affect Epo's specific bioactivity (15) (data not shown). WT and R103A Epo monomer and dimer samples estimated by RIA to contain the same amounts of Epo were run on a denaturing SDS-polyacrylamide gel, and blotted with monoclonal antibodies against the poly-His tag (Fig. 5). For Epo monomers, the density scan of the blot agreed well with the RIA units (within a factor of two), consistent with a previous study which demonstrated by use of conformation-sensitive antibodies that the Arg^{103} → Ala mutation has no apparent effect on the overall folding of Epo (20, 25). The RIA underestimated the concentration of WT dimers by a factor of 2–5. This may explain why the WT dimer appeared to be slightly more active than Arg^{103} dimer in our bioassay (Fig. 2). Poly-His-tagged R103A dimer had approximately the same Western blot signal as that of the two monomers (Fig. 5). Thus our estimate of the specific bioactivity of dimeric R103A is not confounded by use of excessive protein, and can be confidently attributed to the presence of the second monomer.

DISCUSSION

The simplest explanation of the results in Figs. 2–4 is that the dimeric R103A Epo has two active receptor binding domains, each from one R103A monomeric unit. They each bind to one EpoR molecule, and bring them into close enough proximity to enable activation. Thus the deficient receptor binding domain in R103A can be compensated by the active binding site of a second R103A Epo which is covalently linked in the dimer construction.

In principle, parallel experiments could be performed with monomeric and dimeric mutants at positions 150–152, the sites on helix D that have been proposed to comprise an independent receptor-binding domain. However, in contrast to

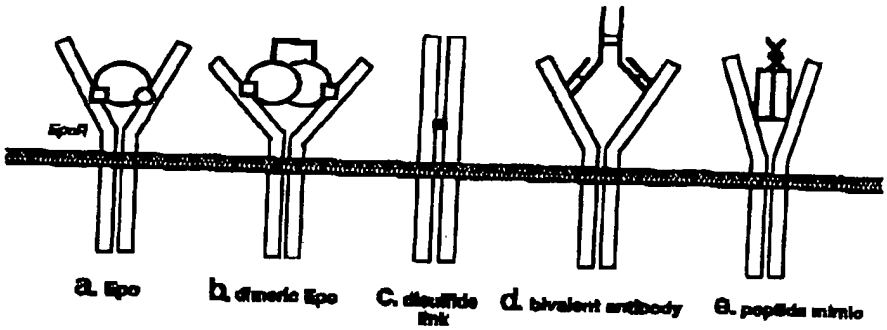

FIG. 6. Schematic presentation of different molecular mechanisms which can induce Epo receptor activation. The two receptor binding domains of Epo are depicted by a *rectangle* and a *circle*.

R103A which is completely "dead," the mutants on helix D that have been studied so far (18–20) show either impaired folding into native tertiary structure or only partial diminution of specific biological activity. Therefore, data obtained from homodimers of these mutants would be difficult to interpret.

Interestingly, the wild-type monomeric Epo is significantly more active than the wild-type dimer and R103A dimer. Although more sophisticated quantitation is required to address this question, one possible explanation is that the dimeric Epo molecules impose steric hindrance when binding to receptor, resulting a lower binding affinity. The dose dependence curves of R103A dimer (Fig. 2) are slightly steeper than those of both monomeric and dimeric Epo, suggesting possible cooperativity. This is consistent with the current model of Epo function (19) in which the R103A dimer would be composed of two tight binding sites, and thus recruitment of the second receptor would be more efficient than with the proposed weak secondary binding site in wild-type Epo.

Our experiments comparing monomeric and dimeric R103A clearly indicate that two domains (motifs) on the Epo molecule are required for its biological function and strongly support the binding of a single molecule of Epo to two receptor molecules. As shown in Fig. 6, two receptors can be brought into juxtaposition for activation by five different mechanisms: (*a*) a single native Epo molecule containing two different and independent receptor binding motifs (18–20); (*b*) as shown in this study, a dimeric Epo, containing only one binding motif on each monomer; (*c*) a mutant EpoR which is cross-linked via a disulfide bond; (*d*) a bifunctional antibody against the extracellular portion of the Epo receptor (8, 9); and (*e*) an EpoR-binding mimetic peptide (13, 14). The length of linker in the dimeric Epo does not seem to be important (Figs. 2 and 3). Mutant dimers having spacers of 3, 5, or 7 glycine residues all gave similar results. A ligand can be effective as long as it has two recognition/binding motifs in the same monomeric molecule, or one motif in each subunit of a dimer.

The mimetic peptide binds to two EpoR molecules as a homodimer; thus the complex has 2–2 stoichiometry and almost perfect 2-fold symmetry (13, 14). It follows that the EpoR-Epo dimer complex reported here should also have 2-fold symmetry. However, native Epo monomers are nonsymmetrical, and Epo's two receptor binding sites appear to have different affinities for EpoR (19). It will be of interest to see whether the nonsymmetric Epo molecule interacts with other accessory proteins. Additional Epo receptor subunits have been proposed (27–30), but not yet characterized. In the absence of high resolution structure of the Epo-EpoR complex, there is the formal possibility that the two domains of Epo have different functions. For example the domain that includes Arg^{103} may bind to another Epo molecule or to an accessory protein, and thus indirectly interacts with the Epo receptor.

The design and evaluation of peptide-linked homodimers may be applied to other cytokines or growth factors whose signaling function depends on bringing receptor subunits into apposition. Synthetic molecules (for bioavailability) or large protein molecules (for enhanced activity or stability) can be evaluated as replacements for the native proteins currently in clinical use.

REFERENCES

1. Cunningham, B. C., Jhurani, P., Ng, P., and Wells, J. A. (1989) *Science* **243**, 1330–1336
2. deVos, A. M., Ultsch, M., and Kossiakoff, A. A. (1992) *Science* **255**, 306–312
3. Wells, J. A., and Vos, A. M. d. (1993) *Annu. Rev. Biophys. Biomol. Struct.* **22**, 329–351
4. Wells, J. A. (1994) *Curr. Opin. Cell Biol.* **6**, 163–173
5. Harding, P. A., Wang, X., Ohada, S., Chen, W. Y., Wan, W., and Kapchick, J. J. (1996) *J. Biol. Chem.* **271**, 6708–6712
6. Watowich, S., Yoshimura, A., Longmore, G., Hilton, D., Yoshimura, Y., and Lodish, H. (1992) *Proc Natl Acad Sci U. S. A.* **89**, 2140–2144
7. Watowich, S. S., Hilton, D. S., and Lodish, H. F. (1994) *Mol. Cell. Biol.* **14**, 3535–3549
8. Elliott, S., Lorenzini, T., Yanagihara, D., Chang, D., and Elliott, G. (1996) *J. Biol. Chem.* **271**, 24691–24697
9. Schneider, H., Chaovapong, W., Matthews, D., Karkaria, C., Cass, R. T., Zhan, H., Boyle, M., Lorenzini, T., Elliott, S. G., and Giebel, L. B. (1997) *Blood* **89**, 473–482
10. Lodish, H. F., Hilton, D. J., Klingmuller, U., Watowich, S. S., and Wu, H. (1995) *Cold Spring Harbor Symp. Quant. Biol.* **60**, 93–104
11. Damen, J. E., and Krystal, G. (1996) *Exp. Hematol.* **24**, 1455–1459
12. Longmore, G. D., and Lodish, H. F. (1991) *Cell* **67**, 1089–1102
13. Wrighton, N. C., Farrell, F. X., Chang, R., Kashyap, A. K., Barbone, F. P., Mulcahy, L. S., Johnson, D. L., Barrett, R. W., Jolliffe, L. K., and Dower, W. J. (1996) *Science* **273**, 458–463
14. Livnah, O., Stura, E. A., Johnson, D. L., Middleton, S. A., Mulcahy, L. S., Wrighton, N. C., Dower, W. J., Jolliffe, L. K., and Wilson, I. A. (1996) *Science* **273**, 464–471
15. Boissel, J.-P., Lee, W.-R., Presnell, S. R., Cohen, F. E., and Bunn, H. F. (1993) *J. Biol. Chem.* **268**, 15983–15993
16. Bazan, J. F. (1990) *Immunol. Today* **11**, 350–354
17. Grodberg, J., Davis, K. L., and Sythowski, A. J. (1993) *Eur. J. Biochem.* **218**, 597–601
18. Wen, D., Boissel, J.-P., Showers, M., Ruth, B. C., and Bunn, H. P. (1994) *J. Biol. Chem.* **269**, 23839–23846
19. Matthews, D. J., Topping, R. S., Cass, R. T., and Giebel, L. B. (1996) *Proc. Natl. Acad. Sci. U. S. A.* **93**, 9471–9476
20. Elliott, S., Lorenzini, T., Chang, D., Barzilay, J., and Delorme, E. (1997) *Blood* **89**, 493–502
21. Goldberg, M. A., Glass, G. A., Cunningham, J. M., and Bunn, H. P. (1987) *Proc. Natl. Acad. Sci. U. S. A.* **84**, 7972–7976
22. Komatsu, Yamamoto, M., Fujita, H., Miwa, A., Hataka, K., Endo, T., Okano, H., Kataoka, T., Fukumaki, Y., Sasaa, S., and Miura, Y. (1993) *Blood* **82**, 456–464
23. Krystal, G. (1983) *Exp. Hematol.* **11**, 649–660
24. Elliott, S., Chang, D., Delorme, E., Dunn, C., Egrie, J., Griffin, J., Lorenzini, T., Talbot, C., and Hesterberg, L. (1996) *Blood* **87**, 2714–2722
25. Elliott, S., Lorenzini, T., Chang, D., Barzilay, J., Delorme, E., Giffin, J., and Hesterberg, L. (1996) *Blood* **87**, 2702–2713
26. Witthuhn, B., Quelle, F. W., Silvennoinen, O., Yi, T., Tang, B., Miura, O., and Ihle, J. N. (1993) *Cell* **74**, 227–236
27. Mayeux, P., Lacombe, C., Casadevall, N., Chretien, S., Dusanter, L., and Gisselbrecht, S. (1991) *J. Biol. Chem.* **266**, 23380–23385
28. Dong, Y. J., and Goldwasser, E. (1993) *Exp. Hematol.* **21**, 483–486
29. Miura, O., and Ihle, J. N. (1993) *Blood* **81**, 1739–1744
30. Miura, O., and Ihle, J. N. (1993) *Arch. Biochem. Biophys.* **306**, 200–205

This Page is Inserted by IFW Indexing and Scanning Operations and is not part of the Official Record

BEST AVAILABLE IMAGES

Defective images within this document are accurate representations of the original documents submitted by the applicant.

Defects in the images include but are not limited to the items checked:

- ☐ BLACK BORDERS
- ☐ IMAGE CUT OFF AT TOP, BOTTOM OR SIDES
- ☐ FADED TEXT OR DRAWING
- ☐ BLURRED OR ILLEGIBLE TEXT OR DRAWING
- ☐ SKEWED/SLANTED IMAGES
- ☐ COLOR OR BLACK AND WHITE PHOTOGRAPHS
- ☐ GRAY SCALE DOCUMENTS
- ☐ LINES OR MARKS ON ORIGINAL DOCUMENT
- ☐ REFERENCE(S) OR EXHIBIT(S) SUBMITTED ARE POOR QUALITY
- ☐ OTHER: _____

IMAGES ARE BEST AVAILABLE COPY.

As rescanning these documents will not correct the image problems checked, please do not report these problems to the IFW Image Problem Mailbox.